Second Electron-Ion Collider Workshop
Jefferson Lab, March 15th 2004

Evolution Equations of QCD in the Non-Linear Saturation Region

Néstor Armesto

Department of Physics, Theory Division, CERN

1. Introduction.
2. Formalism.
3. The Balitsky-Kovchegov equation: features of the solutions.
4. Consequences in eA and HIC.
5. Summary.

Also talks by M. Baker, V. Guzey, J. Jalilian-Marian, A. H. Mueller and K. Tuchin.

1. Introduction (I):

- Experimentally $xG(x,Q^2) \propto x^{-\lambda}$, $\lambda \sim 0.3 \Longrightarrow$ at small x (large energies), high partonic densities $\Longrightarrow$ saturation: parton densities cannot grow forever (parton fusion balances parton splitting if $A_\mu \propto 1/g$ $\Rightarrow$ non-linear process).

1. Introduction (I):

• Experimentally $xG(x, Q^2) \propto x^{-\lambda}$, $\lambda \sim 0.3 \Longrightarrow$ at small x (large energies), high partonic densities $\Longrightarrow$ saturation: parton densities cannot grow forever (parton fusion balances parton splitting if $A_\mu \propto 1/g$ $\Rightarrow$ non-linear process).

• Appeal:

• Experimentally $xG(x,Q^2) \propto x^{-\lambda}$, $\lambda \sim 0.3 \Longrightarrow$ at small x (large energies), high partonic densities $\Longrightarrow$ saturation: parton densities cannot grow forever (parton fusion balances parton splitting if $A_\mu \propto 1/g$ $\Rightarrow$ non-linear process).

• Appeal:
1) New regime of QCD, with old ideas (pomeron interaction, multiple scattering in Reggeon Field Theory, geometrical cross sections, coherence arguments,. . .) in a new (QCD) language.

1. Introduction (I):

- Experimentally $xG(x,Q^2) \propto x^{-\lambda}$, $\lambda \sim 0.3 \Longrightarrow$ at small x (large energies), high partonic densities $\Longrightarrow$ saturation: parton densities cannot grow forever (parton fusion balances parton splitting if $A_\mu \propto 1/g$ $\Rightarrow$ non-linear process).

- Appeal:

1) New regime of QCD, with old ideas (pomeron interaction, multiple scattering in Reggeon Field Theory, geometrical cross sections, coherence arguments,. . .) in a new (QCD) language.
2) Link of small x Physics and ultrarelativistic nuclear collisions (initial stage of a nuclear collision, enhancement due to nuclear length).

1. Introduction (I):

• Experimentally $xG(x, Q^2) \propto x^{-\lambda}$, $\lambda \sim 0.3 \Longrightarrow$ at small x (large energies), high partonic densities $\Longrightarrow$ saturation: parton densities cannot grow forever (parton fusion balances parton splitting if $A_\mu \propto 1/g$ $\Rightarrow$ non-linear process).

• Appeal:
1) New regime of QCD, with old ideas (pomeron interaction, multiple scattering in Reggeon Field Theory, geometrical cross sections, coherence arguments,. . .) in a new (QCD) language.
2) Link of small x Physics and ultrarelativistic nuclear collisions (initial stage of a nuclear collision, enhancement due to nuclear length).

• Basic aim: to study the formulation and consequences of unitarity in terms of the QCD fields.

1. Introduction (II):

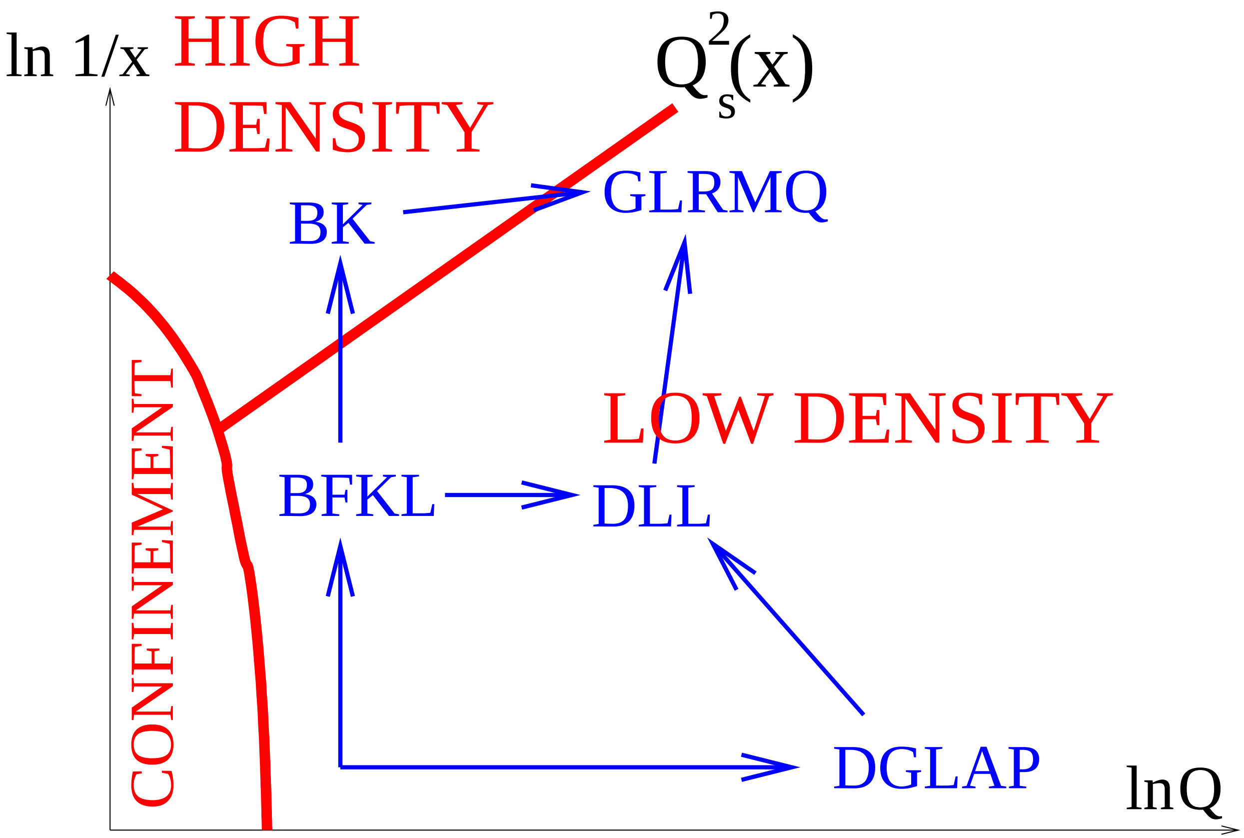

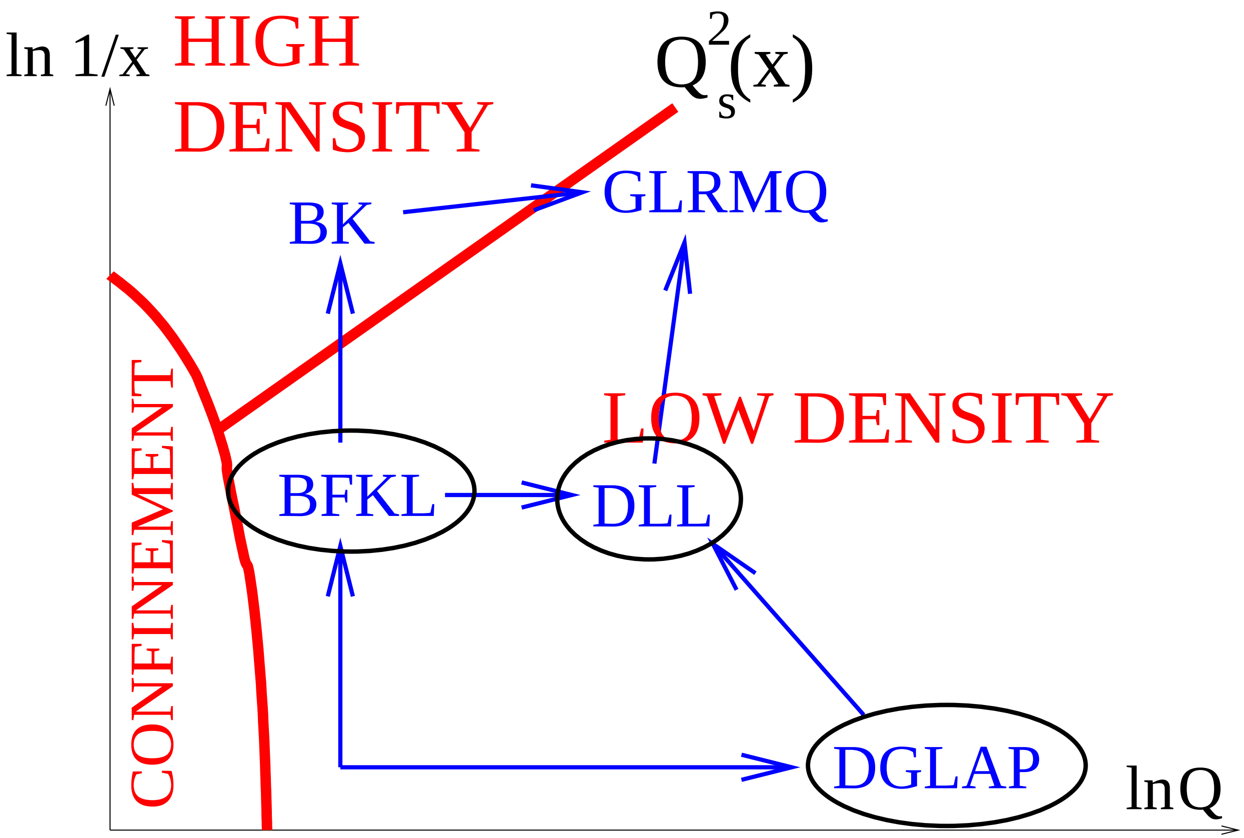

- Linear evolution equations: Dokshitzer-Gribov-Lipatov-Altarelli-Parisi in $\ln Q^2$, Balistky-Fadin-Kuraev-Lipatov in $\ln{(1/x)}$.

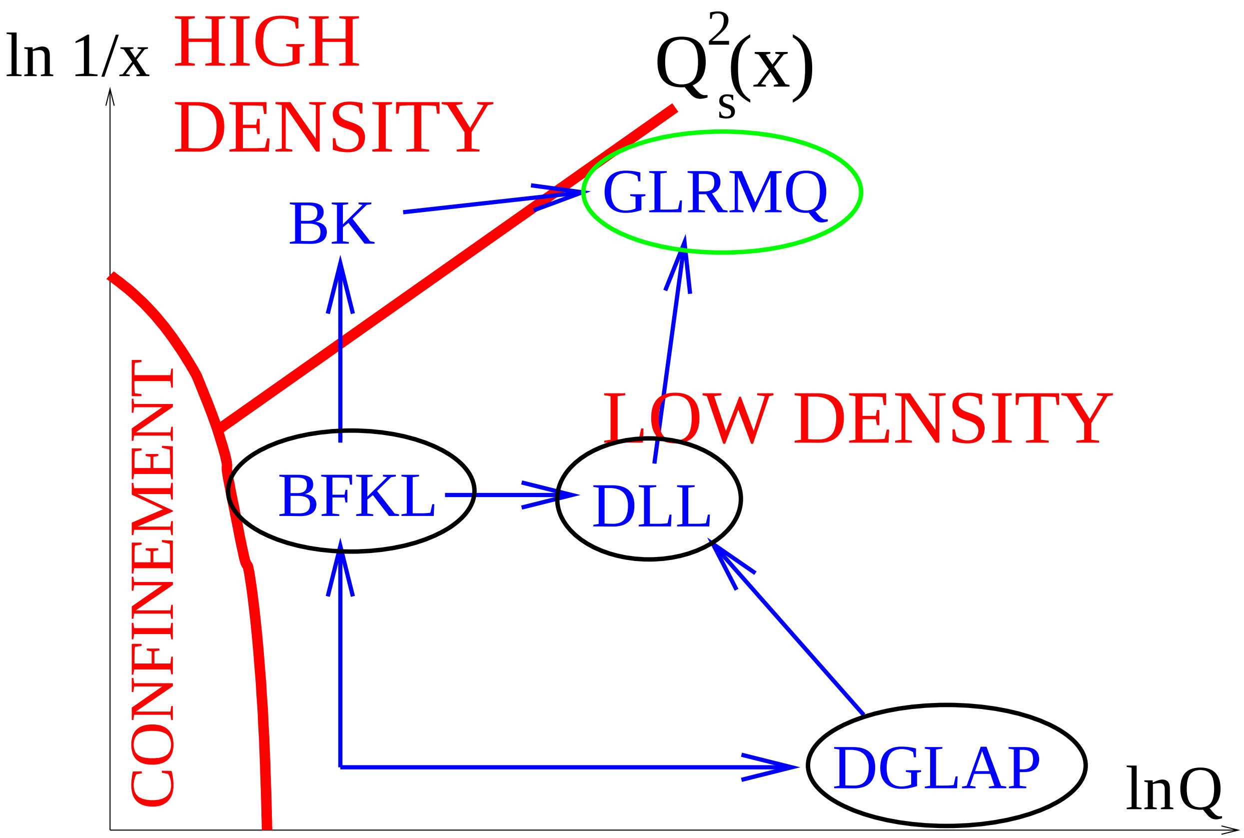

- Linear evolution equations: Dokshitzer-Gribov-Lipatov-Altarelli-Parisi in $\ln Q^2$, Balistky-Fadin-Kuraev-Lipatov in $\ln{(1/x)}$.
- First (twist-four) non-linear correction: Gribov-Levin-Ryskin-Mueller-Qiu in $\ln Q^2$ (GLR, PR100(83)1; MQ, NPB268(86)427).

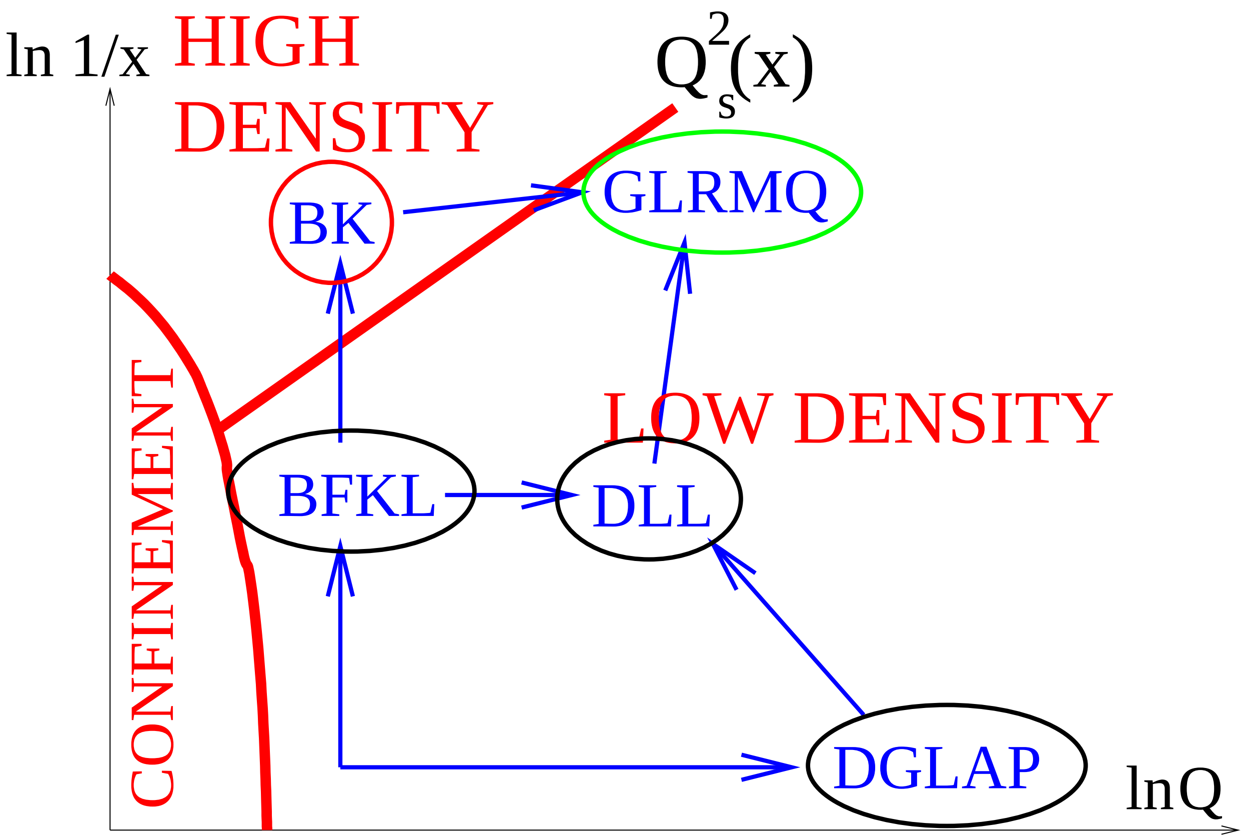

- Linear evolution equations: Dokshitzer-Gribov-Lipatov-Altarelli-Parisi in $\ln Q^2$, Balistky-Fadin-Kuraev-Lipatov in $\ln(1/x)$.
- First (twist-four) non-linear correction: Gribov-Levin-Ryskin-Mueller-Qiu in $\ln Q^2$ (GLR, PR100(83)1; MQ, NPB268(86)427).
- Non-linear, all-twist evolution equation in the saturation region: Balitsky-Kovchegov in $\ln(1/x)$ (B, NPB463(96)99; K, PRD60(99)034008).

2. Formalism (I):

Néstor Armesto

• The McLerran-Venugopalan model (MV, PRD49(94)2233; 3354) treats classical radiation from color sources moving ultrarelativistically through a large nucleus. With a form for the color correlators in the target, a gluon distribution saturated at small $\mathbf{k}_\perp$ is obtained: initial condition.

2. Formalism (I):

- The McLerran-Venugopalan model (MV, PRD49(94)2233; 3354) treats classical radiation from color sources moving ultrarelativistically through a large nucleus. With a form for the color correlators in the target, a gluon distribution saturated at small $\mathbf{k}_\perp$ is obtained: initial condition.
- Later on, gluon radiation (quantum evolution) of the color sources was introduced, which leads to an evolution equation: Color Glass Condensate (JKMW, PRD55(97)5414; ILM, PLB510(01)133). The rescattering of the projectile in the nucleus is described through Wilson lines whose average on target configurations gives the S-matrix (KW, PRD64(01)114002).

2. Formalism (I):

- The McLerran-Venugopalan model (MV, PRD49(94)2233; 3354) treats classical radiation from color sources moving ultrarelativistically through a large nucleus. With a form for the color correlators in the target, a gluon distribution saturated at small $\mathbf{k}_\perp$ is obtained: initial condition.
- Later on, gluon radiation (quantum evolution) of the color sources was introduced, which leads to an evolution equation: Color Glass Condensate (JKMW, PRD55(97)5414; ILM, PLB510(01)133). The rescattering of the projectile in the nucleus is described through Wilson lines whose average on target configurations gives the S-matrix (KW, PRD64(01)114002).
- Key point: fields (occupation numbers) become large ($F_{\mu\nu}, f_g \propto 1/g^2$) $\Rightarrow$ classical arguments, but coupling small $\Rightarrow$ perturbative methods.

2. Formalism (I):

- The McLerran-Venugopalan model (MV, PRD49(94)2233; 3354) treats classical radiation from color sources moving ultrarelativistically through a large nucleus. With a form for the color correlators in the target, a gluon distribution saturated at small $\mathbf{k}_\perp$ is obtained: initial condition.
- Later on, gluon radiation (quantum evolution) of the color sources was introduced, which leads to an evolution equation: Color Glass Condensate (JKMW, PRD55(97)5414; ILM, PLB510(01)133). The rescattering of the projectile in the nucleus is described through Wilson lines whose average on target configurations gives the S-matrix (KW, PRD64(01)114002).
- Key point: fields (occupation numbers) become large ($F_{\mu\nu}, f_g \propto 1/g^2$) $\Rightarrow$ classical arguments, but coupling small $\Rightarrow$ perturbative methods.
- The coupled equations for n-gluon correlators decouple in the large N_c limit: the BK equation appears for $n = 2$; also deduced in BFKL (B, EPJC16(00)337) as a sum of fan diagrams in LL$1/x$ (α_s is fixed).

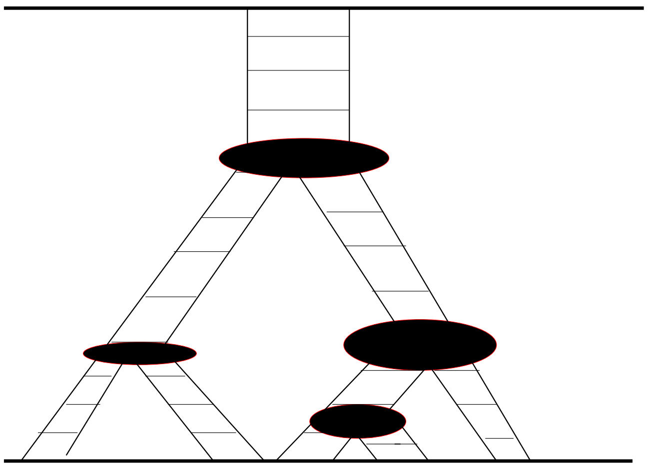

BK equation

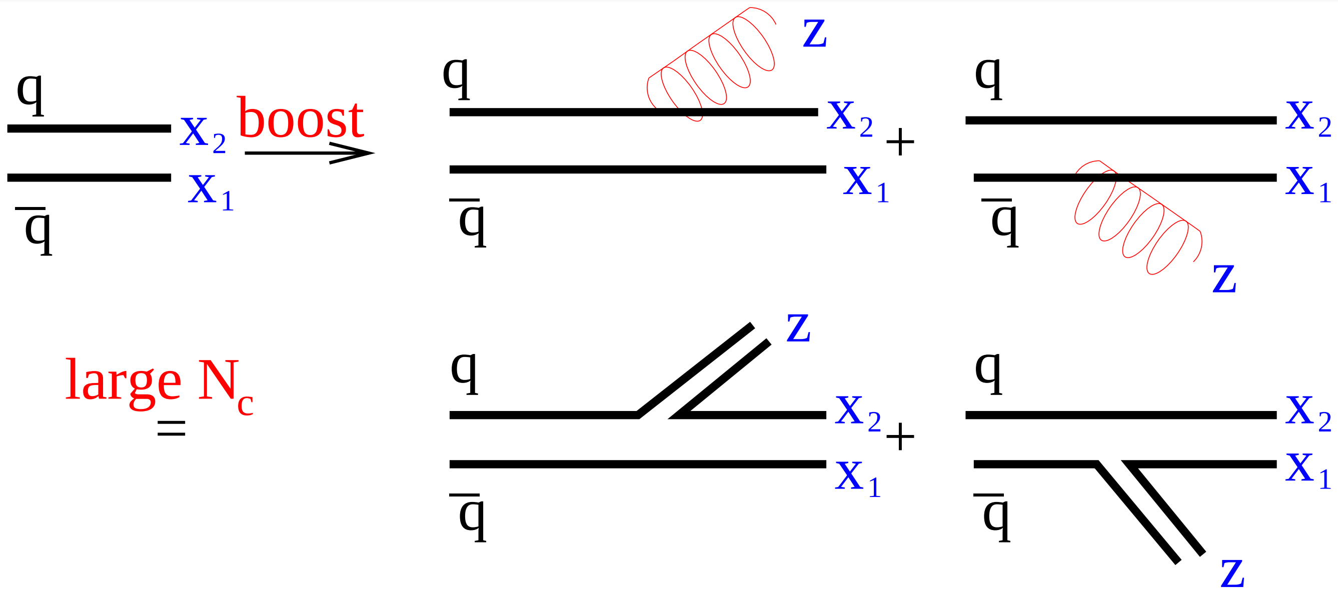

2. Formalism (II):

BK equation

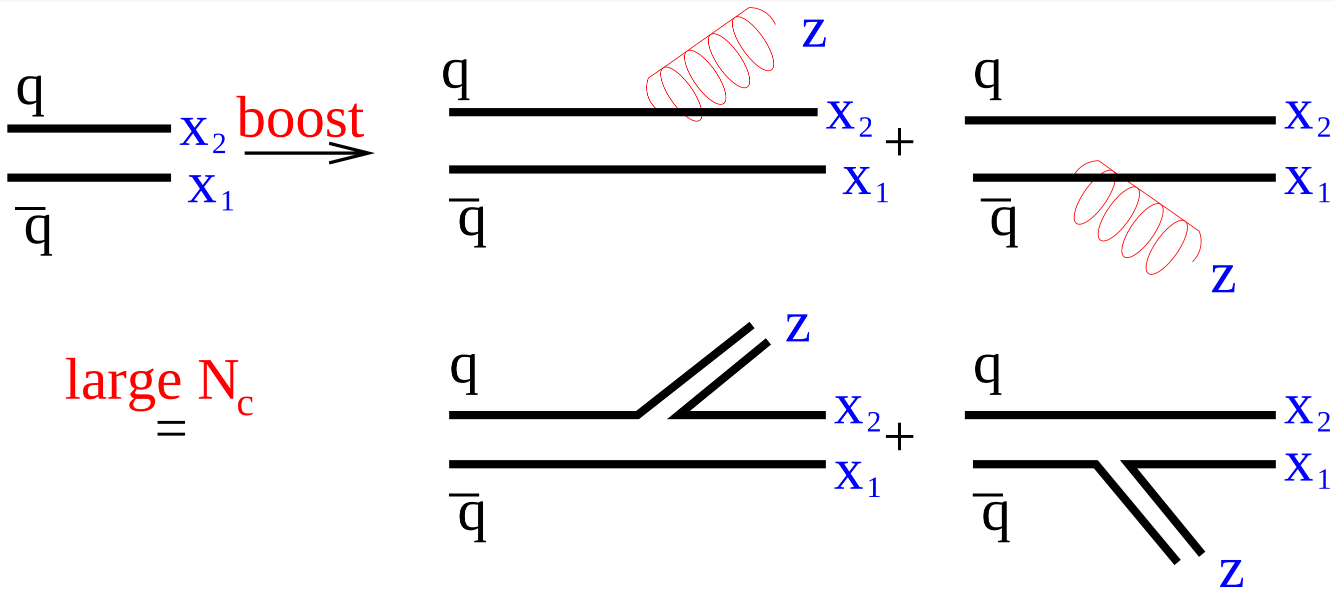

$$Y = \ln(x_0/x), \quad y = \alpha_s N_c Y/\pi, \quad r = x_1 - x_2, \quad b = (x_1 + x_2)/2;$$

2. Formalism (II):

BK equation

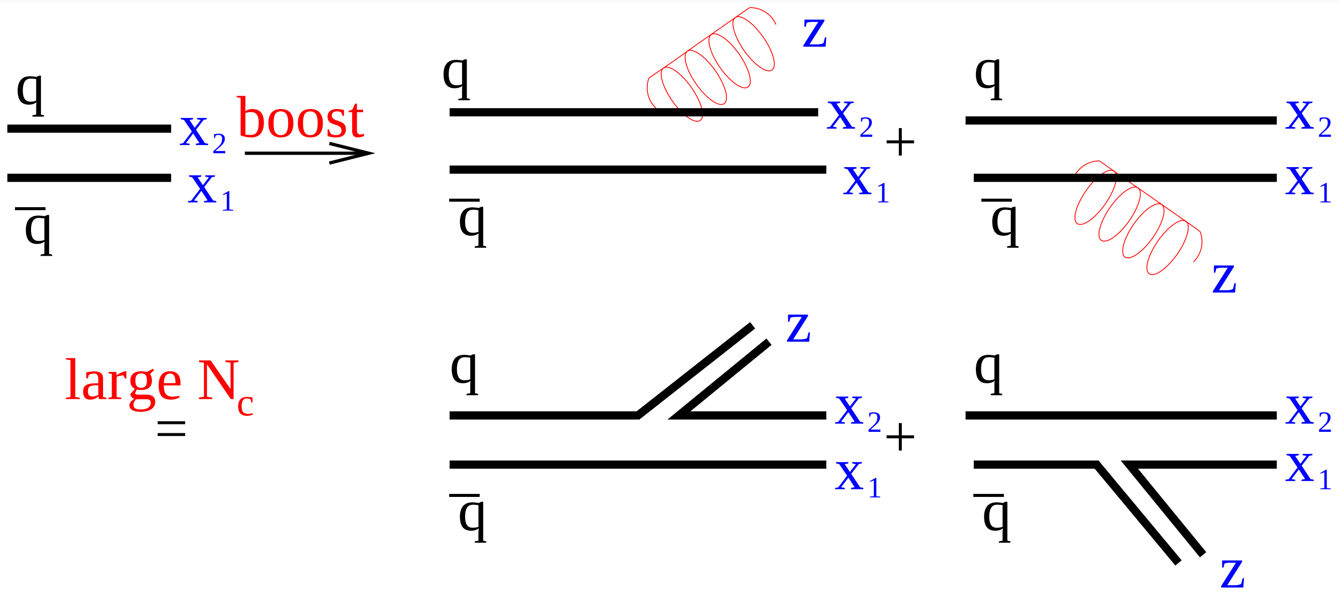

$$Y = \ln(x_0/x), \quad y = \alpha_s N_c Y/\pi, \quad r = x_1 - x_2, \quad b = (x_1 + x_2)/2;$$

$$W_F(x_1, z_+ = 0) = \mathcal{P} e^{ig\int dz_- T^a A_a^+(x_1, z_-)};$$

$$N_{x_1,x_2} = N_c^{-1}\left\langle \mathrm{tr}\left[1 - W_F^\dagger(x_1) W_F(x_2)\right]\right\rangle_t, \quad \phi(k,b) = \int \frac{d^2 r}{2\pi r^2}\, e^{ik\cdot r} N_{x_1,x_2};$$

BK equation

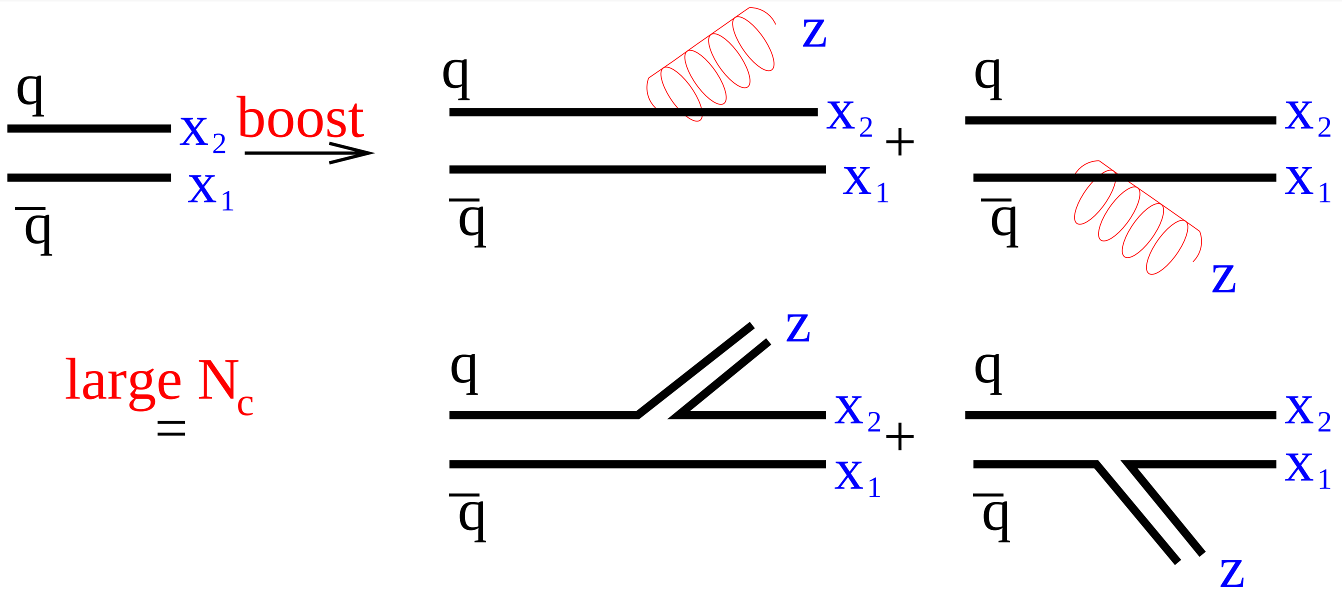

$$Y = \ln(x_0/x), \quad y = \alpha_s N_c Y/\pi, \quad r = x_1 - x_2, \quad b = (x_1 + x_2)/2;$$

$$W_F(x_1, z_+ = 0) = \mathcal{P} e^{ig \int dz_- T^a A_a^+(x_1, z_-)};$$

$$N_{x_1,x_2} = N_c^{-1} \left\langle \mathrm{tr} \left[1 - W_F^\dagger(x_1) W_F(x_2) \right] \right\rangle_t, \quad \phi(k,b) = \int \frac{d^2 r}{2\pi r^2} \, e^{ik \cdot r} N_{x_1,x_2};$$

$$\frac{\partial N_{x_1,x_2}}{\partial Y} = \frac{\alpha_s N_c}{\pi} \int \frac{d^2 z}{2\pi} \frac{(x_1 - x_2)^2}{(x_1 - z)^2 (z - x_2)^2} \left[N_{x_1,z} + N_{z,x_2} - N_{x_1,x_2} \right.$$

BK equation

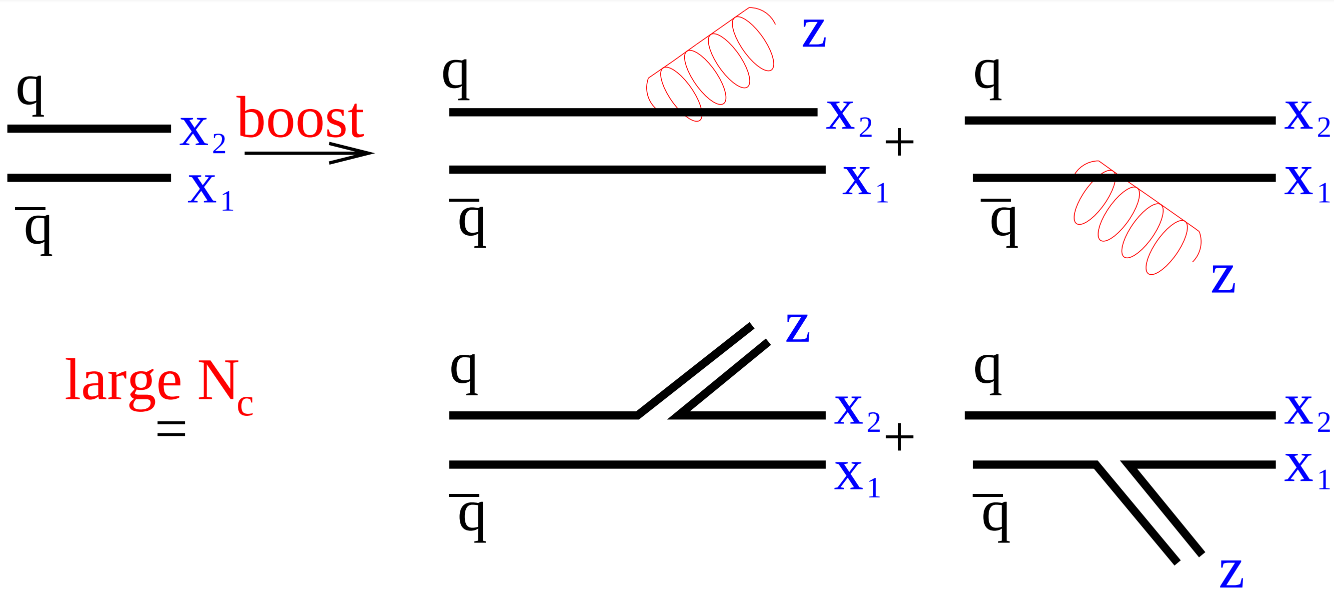

$$Y = \ln(x_0/x), \quad y = \alpha_s N_c Y/\pi, \quad r = x_1 - x_2, \quad b = (x_1 + x_2)/2;$$

$$W_F(x_1, z_+ = 0) = \mathcal{P} e^{ig\int dz_- T^a A_a^+(x_1, z_-)};$$

$$N_{x_1,x_2} = N_c^{-1} \left\langle \mathrm{tr}\left[1 - W_F^\dagger(x_1) W_F(x_2)\right]\right\rangle_t, \quad \phi(k,b) = \int \frac{d^2 r}{2\pi r^2}\, e^{ik\cdot r} N_{x_1,x_2};$$

$$\frac{\partial N_{x_1,x_2}}{\partial Y} = \frac{\alpha_s N_c}{\pi} \int \frac{d^2 z}{2\pi} \frac{(x_1 - x_2)^2}{(x_1 - z)^2 (z - x_2)^2} \left[N_{x_1,z} + N_{z,x_2} - N_{x_1,x_2}\right.$$

$$\left. - N_{x_1,z} N_{z,x_2}\right]$$

2. Formalism (II):

Néstor Armesto

BK equation

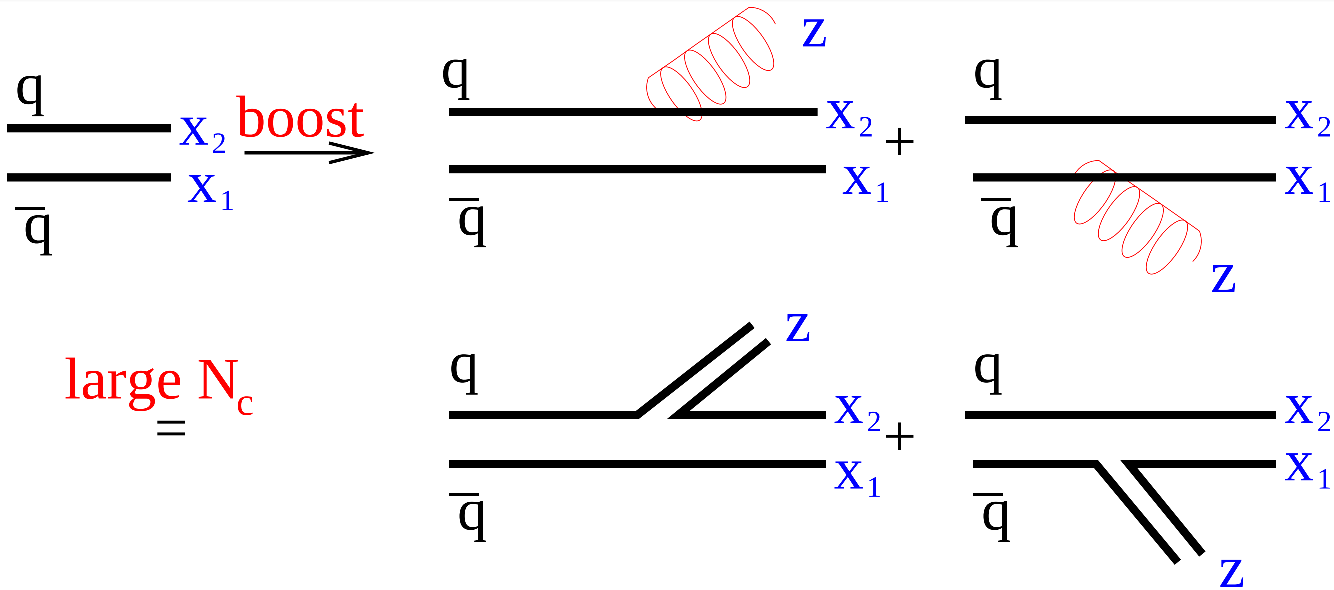

$$Y=\ln(x_0/x),\quad y=\alpha_s N_c Y/\pi,\quad r=x_1-x_2,\quad b=(x_1+x_2)/2;$$

$$W_F(x_1,z_+=0)=\mathcal{P}e^{ig\int dz_- T^a A_a^+(x_1,z_-)};$$

$$N_{x_1,x_2}=N_c^{-1}\left\langle \mathrm{tr}\left[1-W_F^\dagger(x_1)W_F(x_2)\right]\right\rangle_t,\quad \phi(k,b)=\int\frac{d^2r}{2\pi r^2}\,e^{ik\cdot r}N_{x_1,x_2};$$

$$\frac{\partial N_{x_1,x_2}}{\partial Y}=\frac{\alpha_s N_c}{\pi}\int\frac{d^2z}{2\pi}\frac{(x_1-x_2)^2}{(x_1-z)^2(z-x_2)^2}\left[N_{x_1,z}+N_{z,x_2}-N_{x_1,x_2}\right.$$

$$\left.-N_{x_1,z}N_{z,x_2}\right]\longrightarrow\left(\frac{\partial}{\partial y}+H_{\mathrm{BFKL}}\right)\phi(k,b)=-\phi^2(k,b)\ \text{ for }\ b\gg r.$$

3. The Balitsky-Kovchegov equation: features of the solutions:

- Asymptotic integrability.
- Scaling.
- Froissart bound.
- Running coupling.
- Beyond BK.

The analytical solution is unknown: numerical results will be shown and analytical estimations commented.

Asymptotic integrability:

Solutions of BK for $y = 0, 5, 10$ for GBW (solid), and MV with $Q_s = 2$ GeV (dashed) and 10 GeV (dotted) (AAKSW, PRL92(04)082001).

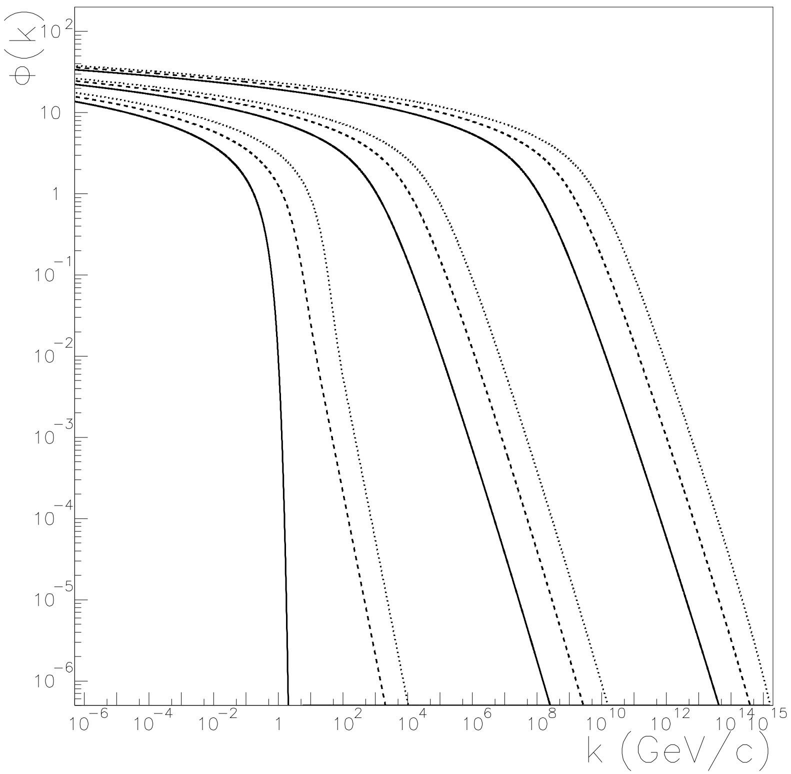

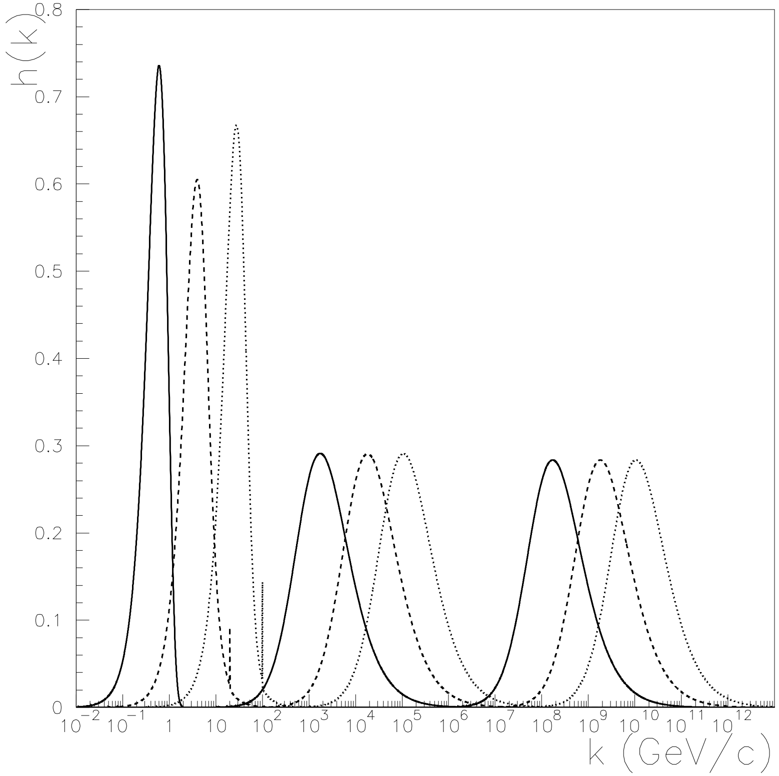

Asymptotic integrability:

Néstor Armesto

Solutions of BK for $y = 0, 5, 10$ for GBW (solid), and MV with $Q_s = 2$ GeV (dashed) and 10 GeV (dotted) (AAKSW, PRL92(04)082001).

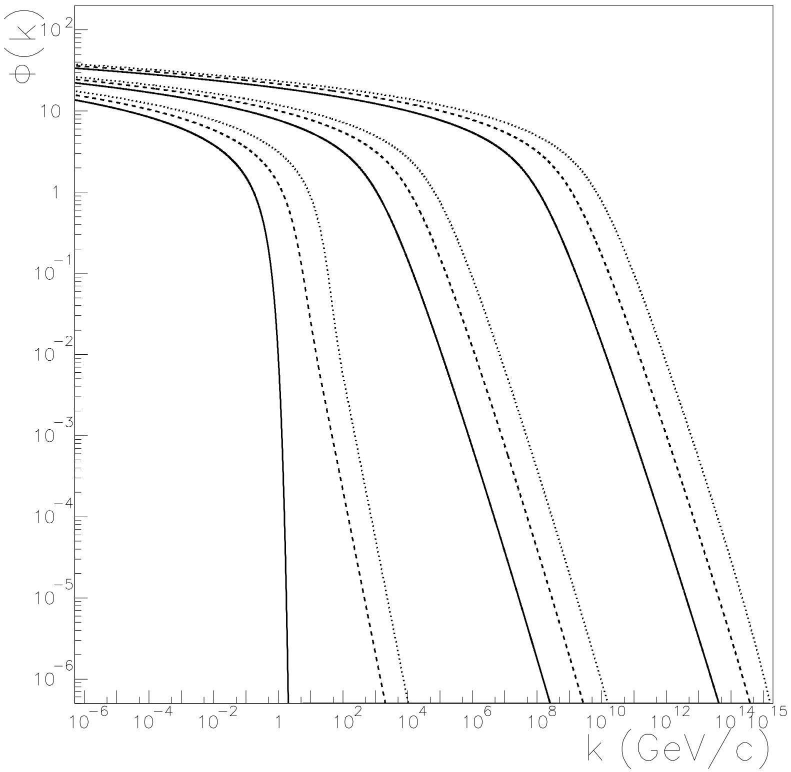

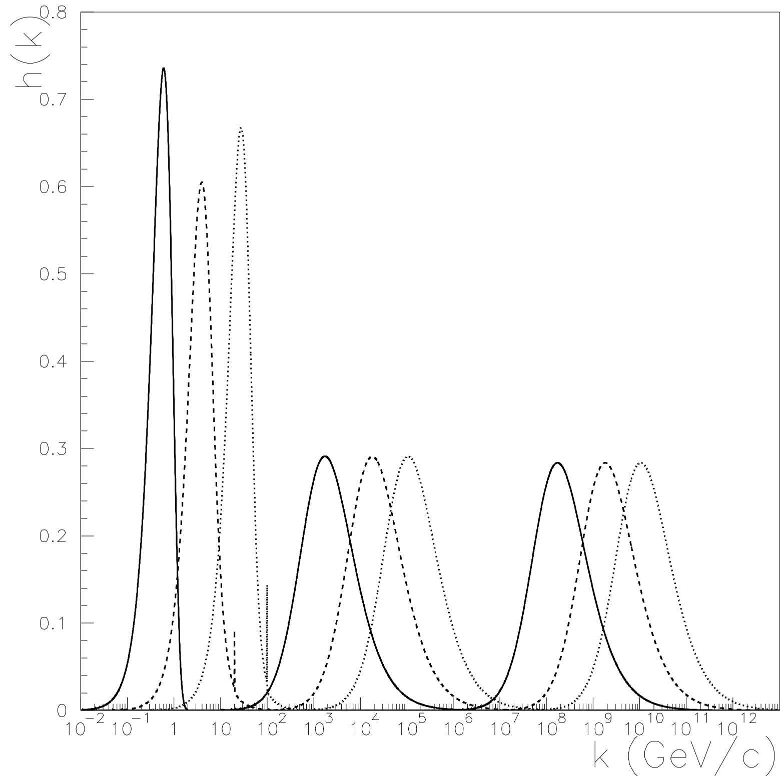

• Solutions tend to a universal shape independent of the initial condition; for $h = k^2\nabla_k^2\phi, \quad \int \frac{d^2k}{2\pi k^2} h(k) = 1$, a soliton-like behavior appears (B, EPJC16(00)337).

Asymptotic integrability:

Solutions of BK for $y = 0, 5, 10$ for GBW (solid), and MV with $Q_s = 2$ GeV (dashed) and 10 GeV (dotted) (AAKSW, PRL92(04)082001).

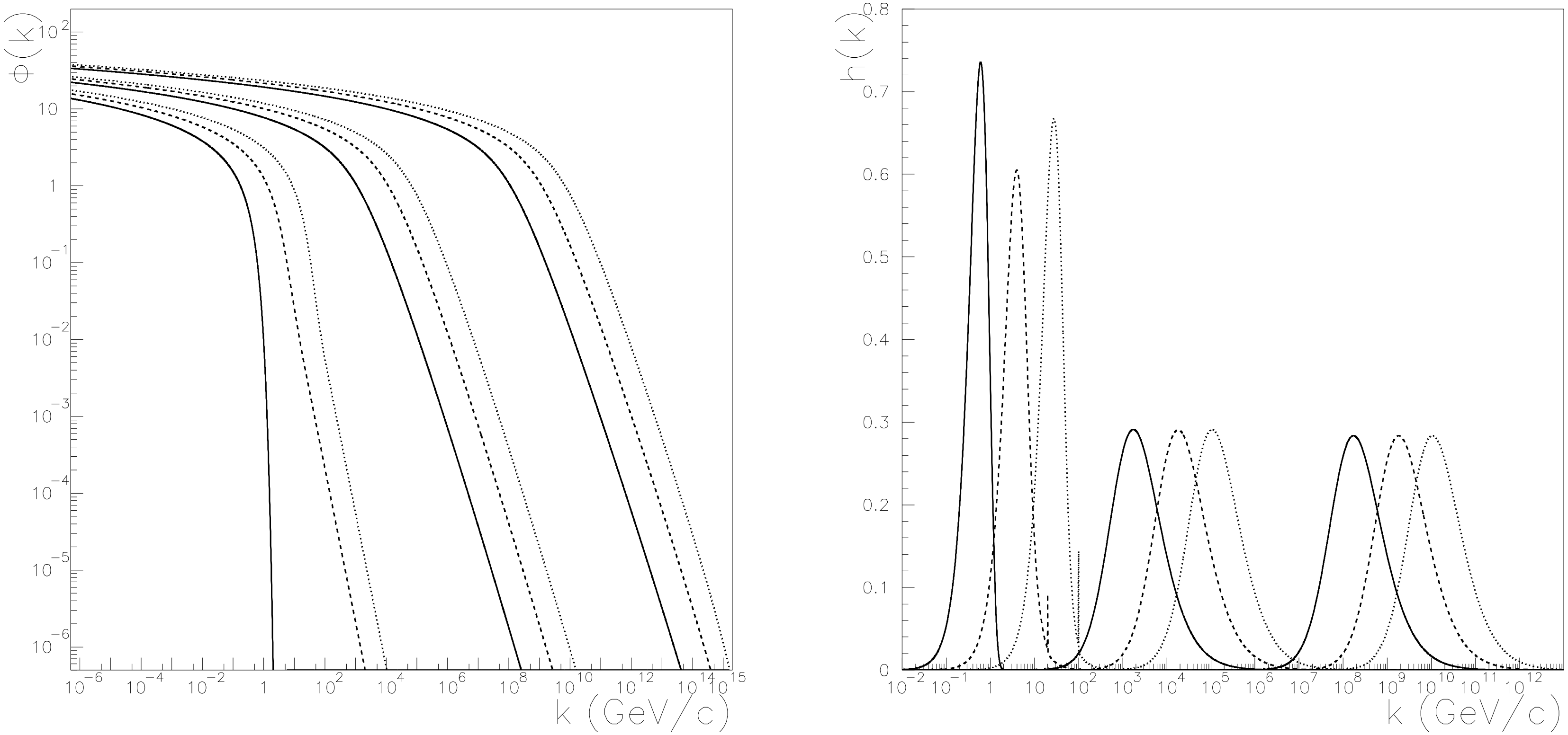

• Solutions tend to a universal shape independent of the initial condition; for $h = k^2 \nabla_k^2 \phi, \quad \int \frac{d^2k}{2\pi k^2} h(k) = 1$, a soliton-like behavior appears (B, EPJC16(00)337).

• Integrability (for $y \to \infty$) has been proved (MP, PRL91(03)232001; hep-ph/0401215).

Asymptotic integrability:

Néstor Armesto

Solutions of BK for $y = 0, 5, 10$ for GBW (solid), and MV with $Q_s = 2$ GeV (dashed) and 10 GeV (dotted) (AAKSW, PRL92(04)082001).

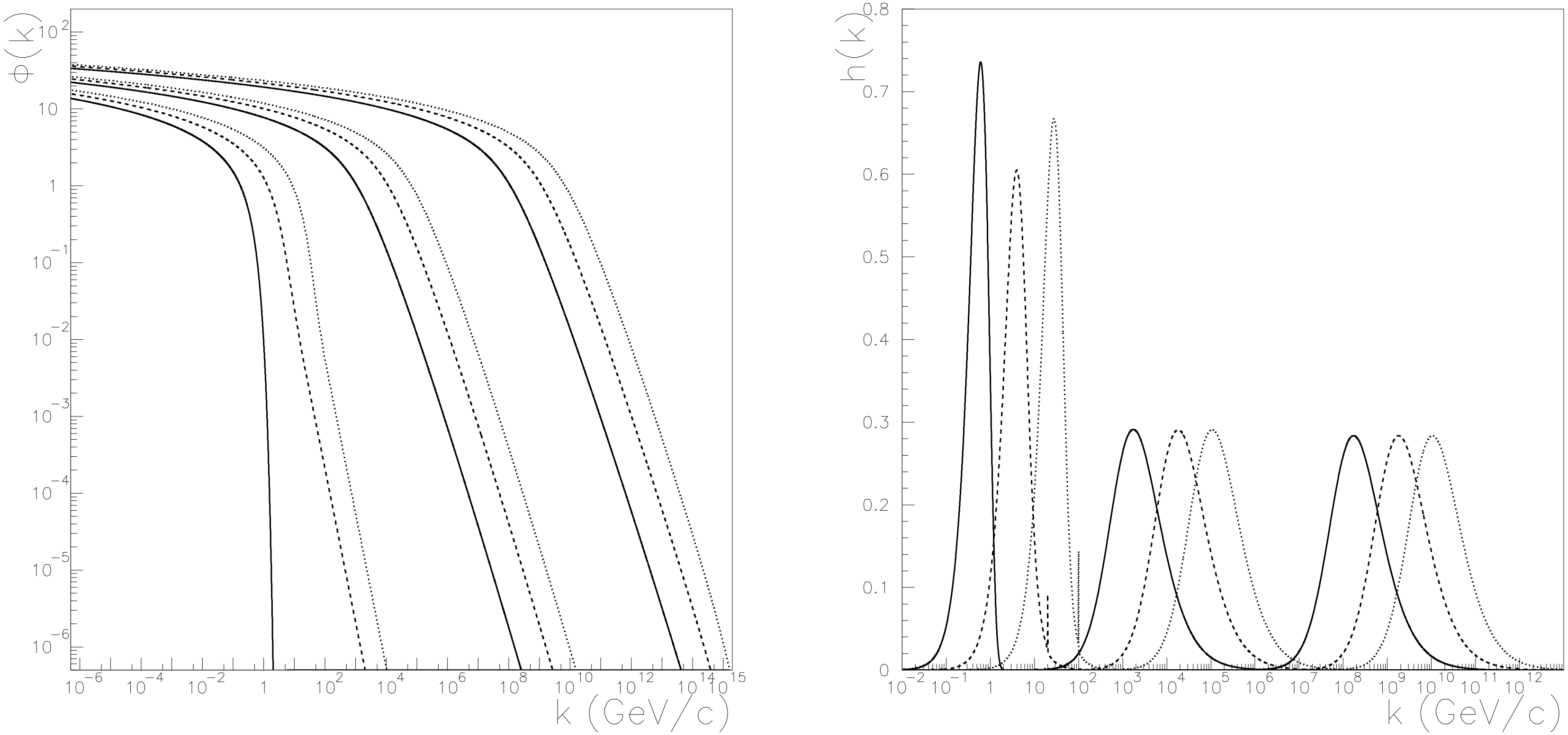

- Solutions tend to a universal shape independent of the initial condition; for $h = k^2 \nabla_k^2 \phi, \quad \int \frac{d^2k}{2\pi k^2} h(k) = 1$, a soliton-like behavior appears (B, EPJC16(00)337).
- Integrability (for $y \to \infty$) has been proved (MP, PRL91(03)232001; hep-ph/0401215).
- Solution to the IR diffusion problem of BFKL (GBMS, PRD65(02)074037).

Solutions of BK for $y = 0, 5, 10$ for GBW (solid), and MV with $Q_s = 2$ GeV (dashed) and 10 GeV (dotted) (AAKSW, PRL92(04)082001).

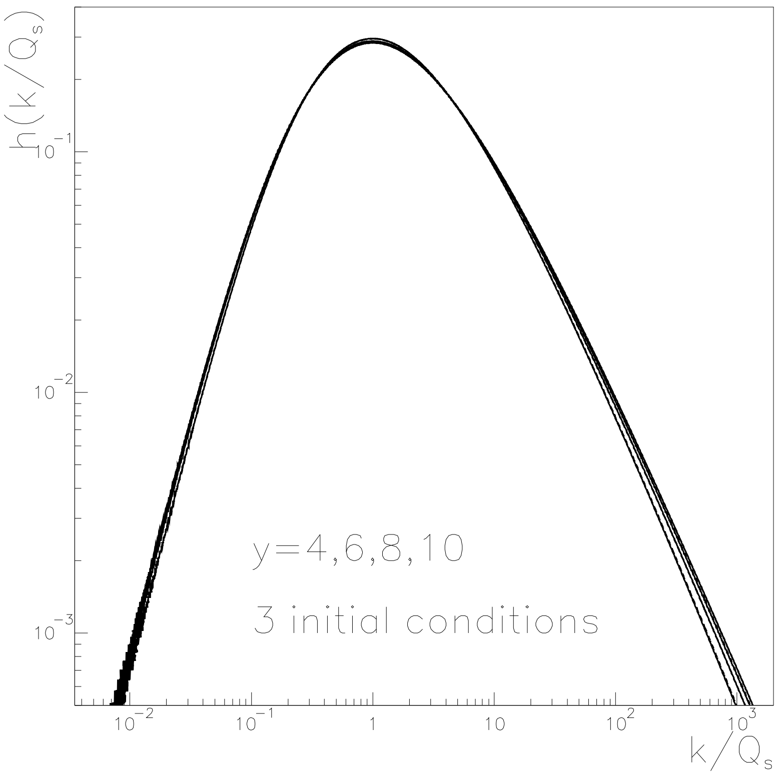

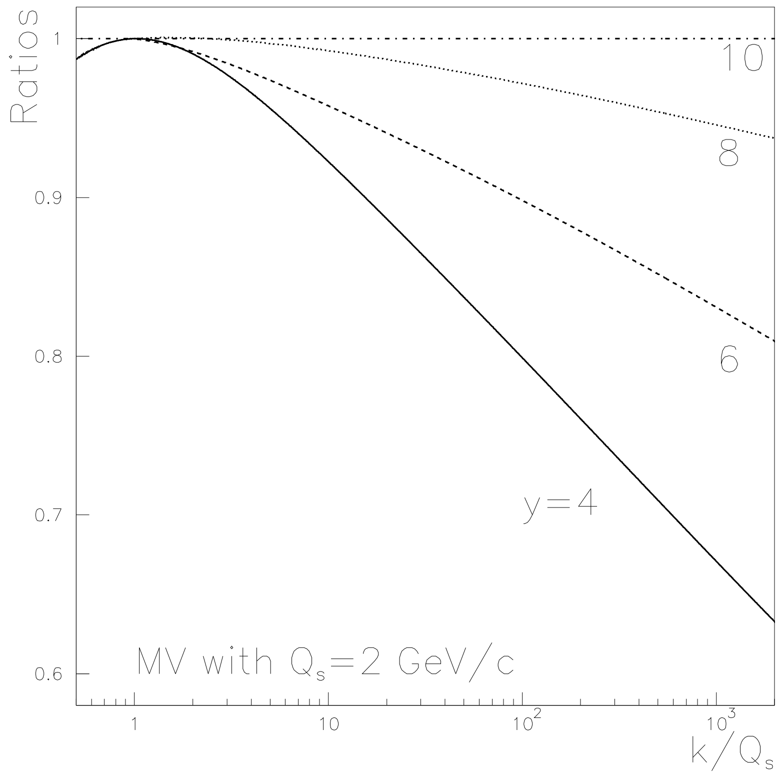

Solutions of BK for $y = 0, 5, 10$ for GBW (solid), and MV with $Q_s = 2$ GeV (dashed) and 10 GeV (dotted) (AAKSW, PRL92(04)082001).

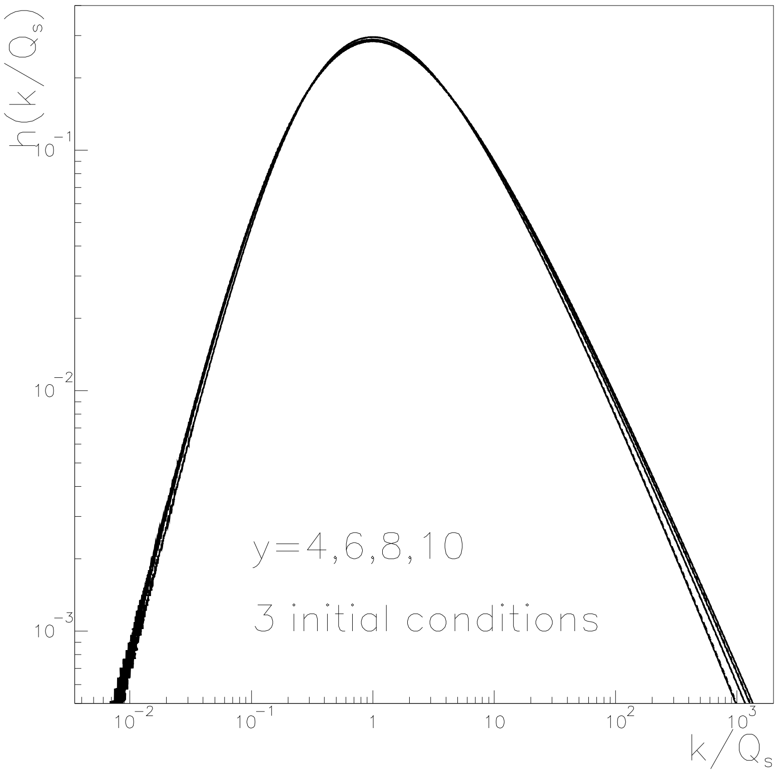

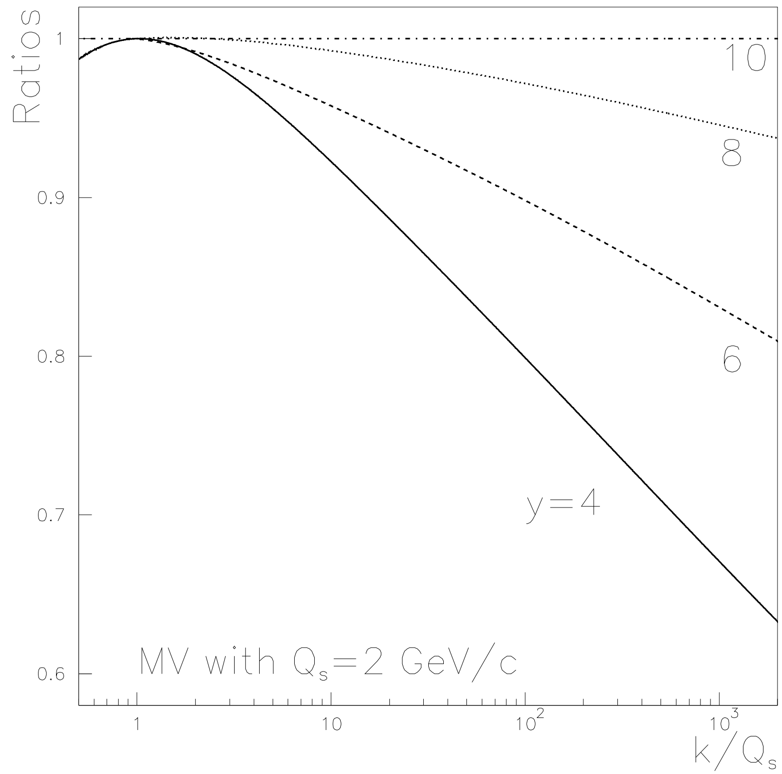

- A universal function of k/Q_s appears (AB, EPJC20(01)517; L, EPJC21(01)513).

Solutions of BK for $y = 0, 5, 10$ for GBW (solid), and MV with $Q_s = 2$ GeV (dashed) and 10 GeV (dotted) (AAKSW, PRL92(04)082001).

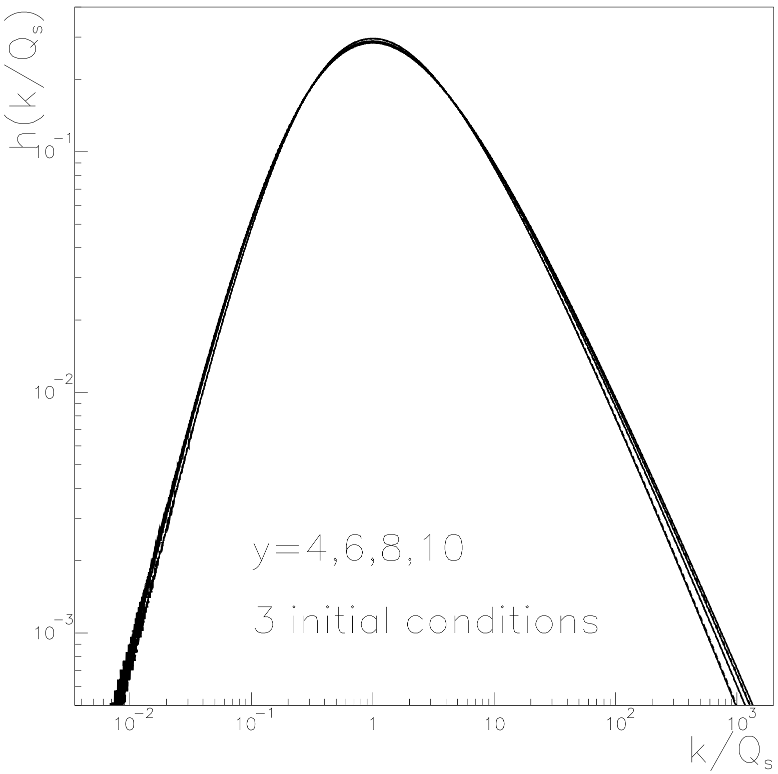

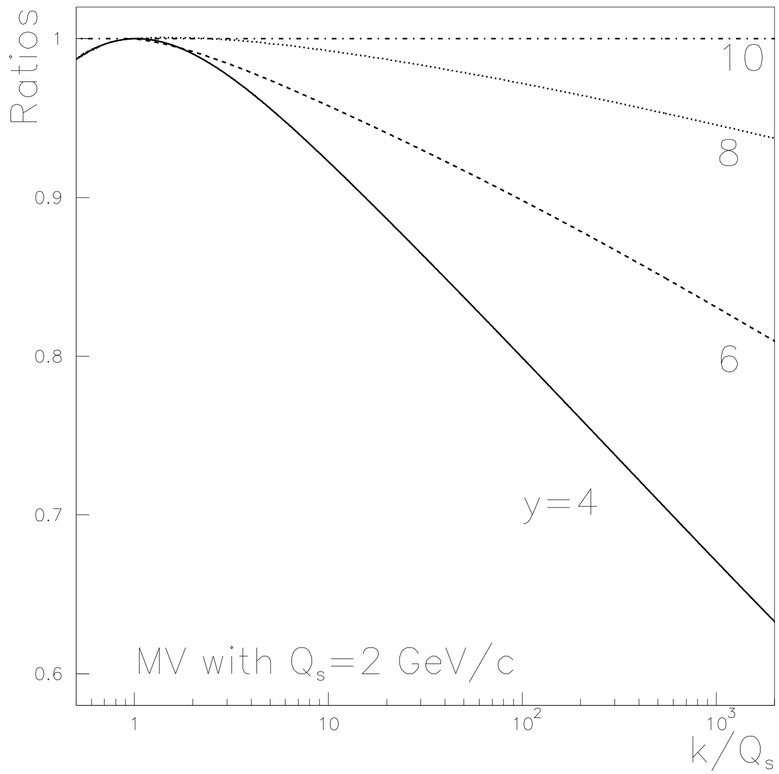

- A universal function of k/Q_s appears (AB, EPJC20(01)517; L, EPJC21(01)513).
- $h(k = Q_s) = h_{\max}$; $Q_s^2(y) \propto A^{\sim 1/3}$ (as expected), and $\propto \exp(\Delta y)$ with $4\ (\mathrm{DLL}) < \Delta < 4.88\ (\mathrm{BFKL})$ (LT, NPB573(00)833; LL, NPA696(01)833).

Solutions of BK for $y = 0, 5, 10$ for GBW (solid), and MV with $Q_s = 2$ GeV (dashed) and 10 GeV (dotted) (AAKSW, PRL92(04)082001).

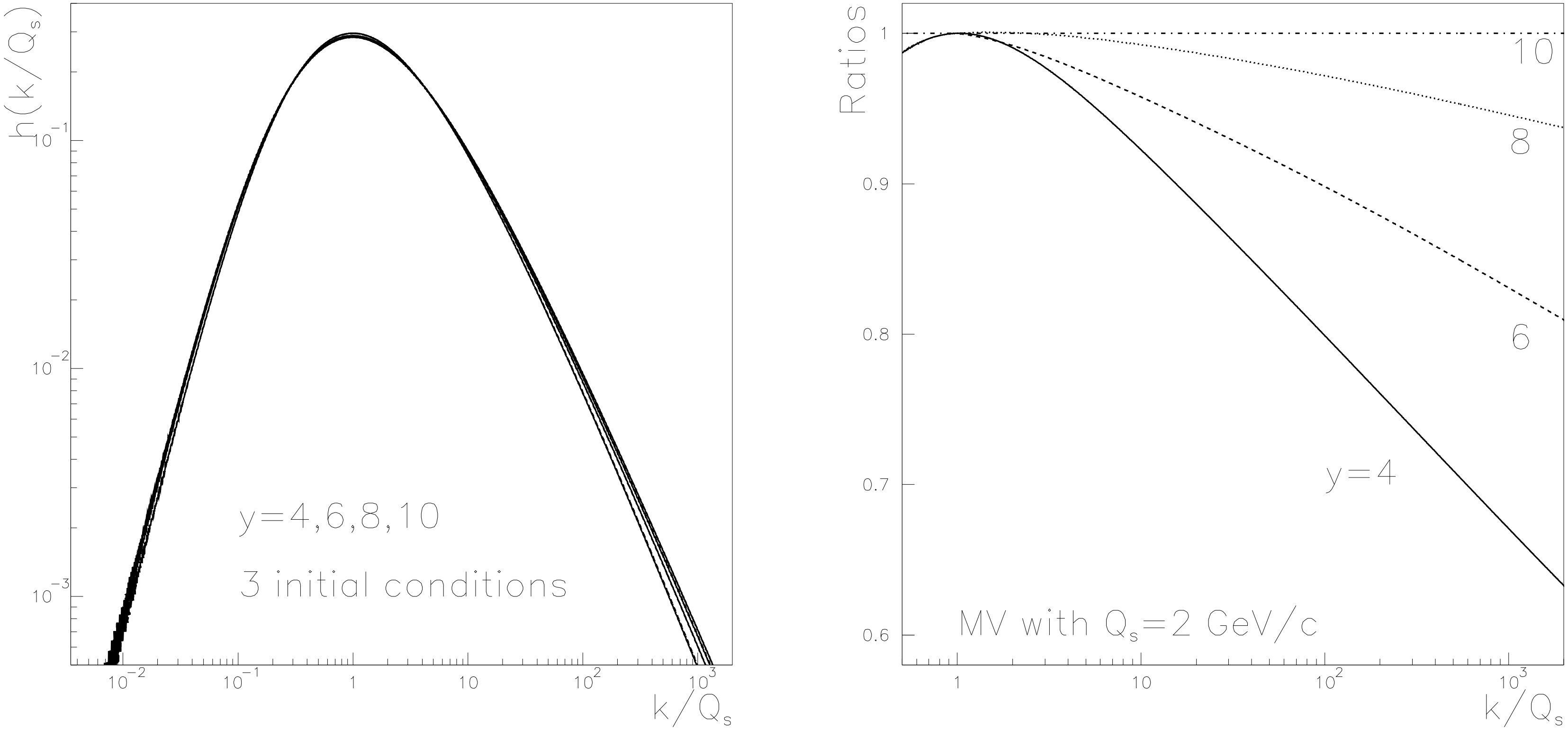

- A universal function of k/Q_s appears (AB, EPJC20(01)517; L, EPJC21(01)513).
- $h(k = Q_s) = h_{\max}$; $Q_s^2(y) \propto A^{\sim 1/3}$ (as expected), and $\propto \exp{(\Delta y)}$ with $4\ (\mathrm{DLL}) < \Delta < 4.88\ (\mathrm{BFKL})$ (LT, NPB573(00)833; LL, NPA696(01)833).
- Scaling observed in l-p (SGBK, PRL86(01)596), l-A? (FRWS, PRL90(03)222002).

Scaling:

Solutions of BK for $y = 0, 5, 10$ for GBW (solid), and MV with $Q_s = 2$ GeV (dashed) and 10 GeV (dotted) (AAKSW, PRL92(04)082001).

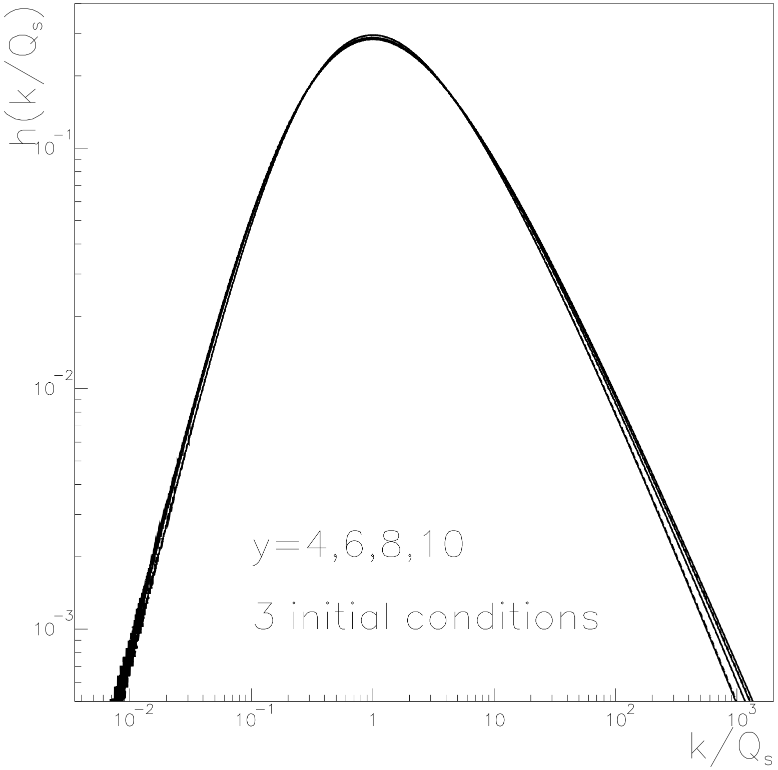

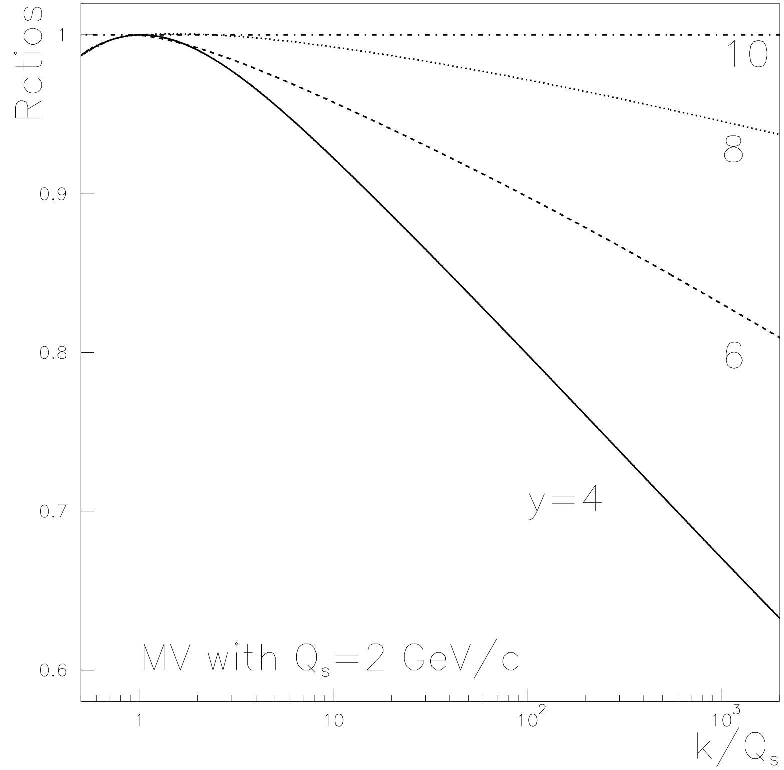

- A universal function of k/Q_s appears (AB, EPJC20(01)517; L, EPJC21(01)513).
- $h(k = Q_s) = h_{\max}$; $Q_s^2(y) \propto A^{\sim 1/3}$ (as expected), and $\propto \exp(\Delta y)$ with $4\ (\mathrm{DLL}) < \Delta < 4.88\ (\mathrm{BFKL})$ (LT, NPB573(00)833; LL, NPA696(01)833).
- Scaling observed in l-p (SGBK, PRL86(01)596), l-A? (FRWS, PRL90(03)222002).
- For $Q_s < k < k_{\mathrm{sw}}(Q_s)$, log corrected shape (MT, NPB640(02)331) favored (AAKSW, PRL92(04)082001) over pure power (IIM, NPA708(02)327).

Solution of BK with b-dependence, for fixed r and angle between **r** and **b** (GBS, NPB668(03)345).

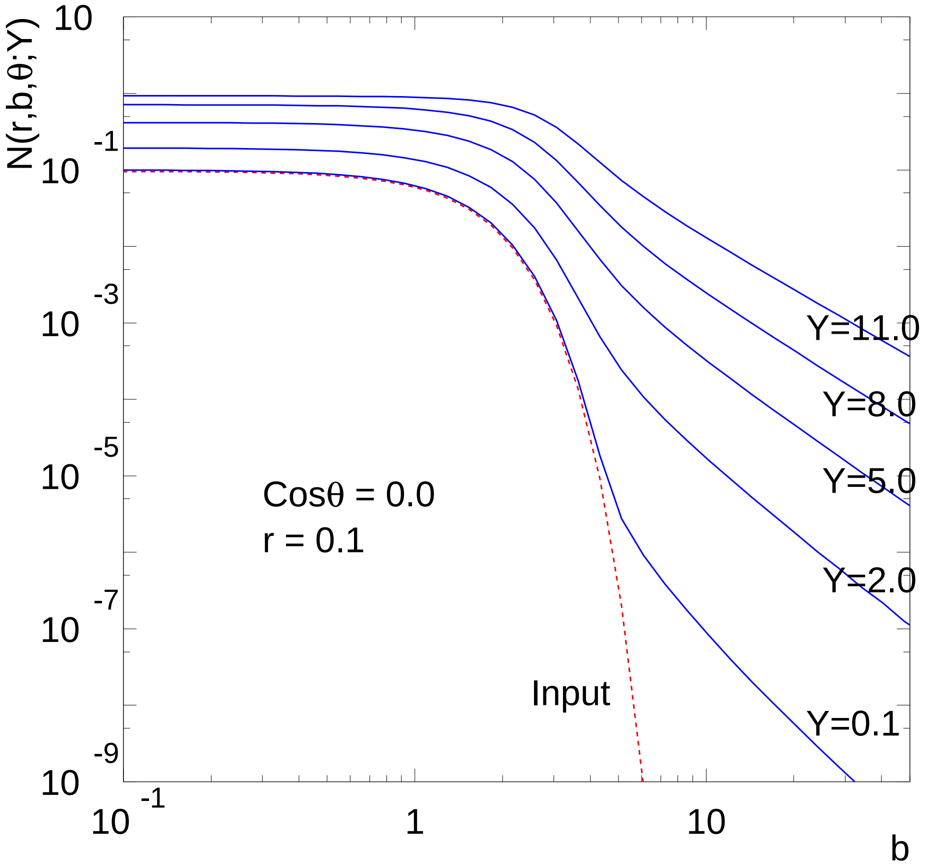

Solution of BK with b-dependence, for fixed r and angle between **r** and **b** (GBS, NPB668(03)345).

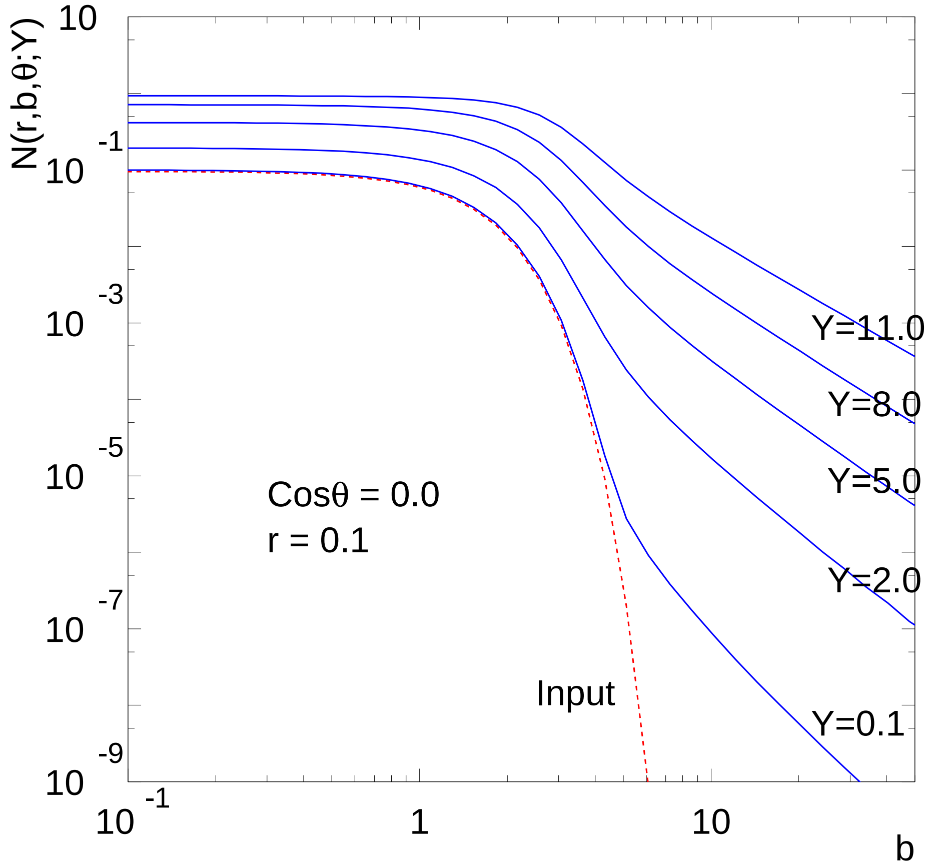

- Froissart bound, $\sigma \propto \ln^2 s$, recovered by non-linear effects? (FIIM, NPA710(01)373; KW, PRD66(02)051502; PLB551(03)311): b-dependence.

Froissart bound:

Solution of BK with b-dependence, for fixed r and angle between **r** and **b** (GBS, NPB668(03)345).

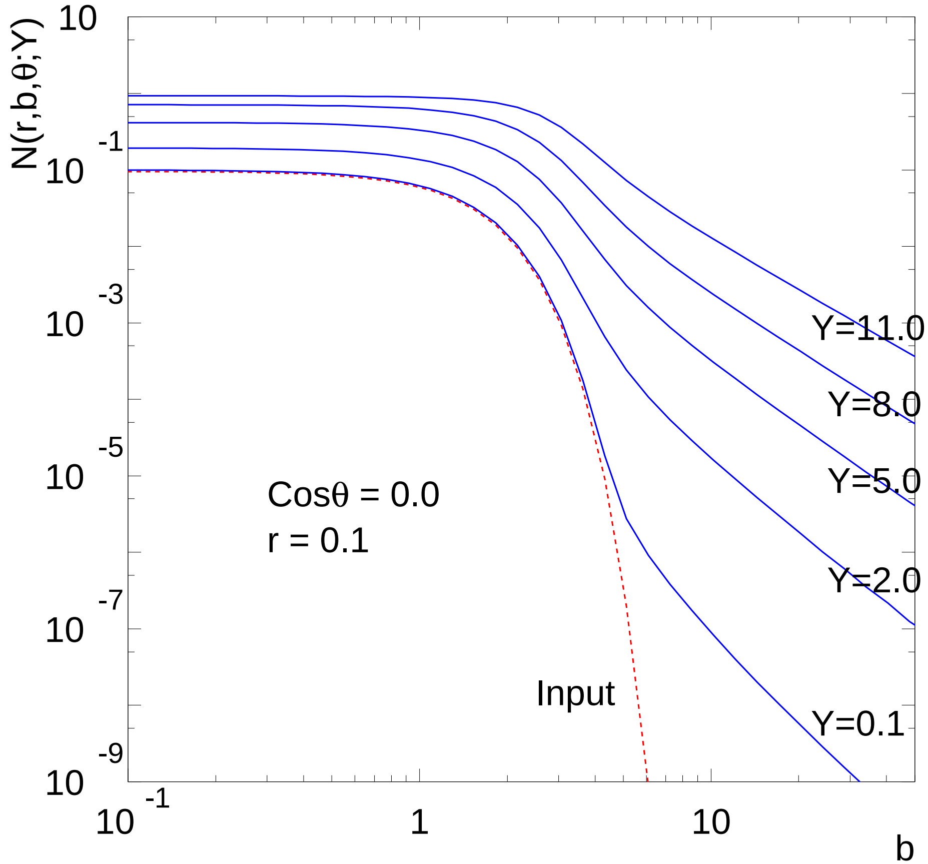

• Froissart bound, $\sigma \propto \ln^2 s$, recovered by non-linear effects? (FIIM, NPA710(01)373; KW, PRD66(02)051502; PLB551(03)311): b-dependence.

• No mass gap $\Rightarrow$ no Froissart expected; initial condition $\propto e^{-Ab}$ for $b \gg$ but a tail $\propto b^{-4}$ develops $\Rightarrow$ regulation of the kernel is demanded.

Solution of BK with b-dependence, for fixed r and angle between **r** and **b** (GBS, NPB668(03)345).

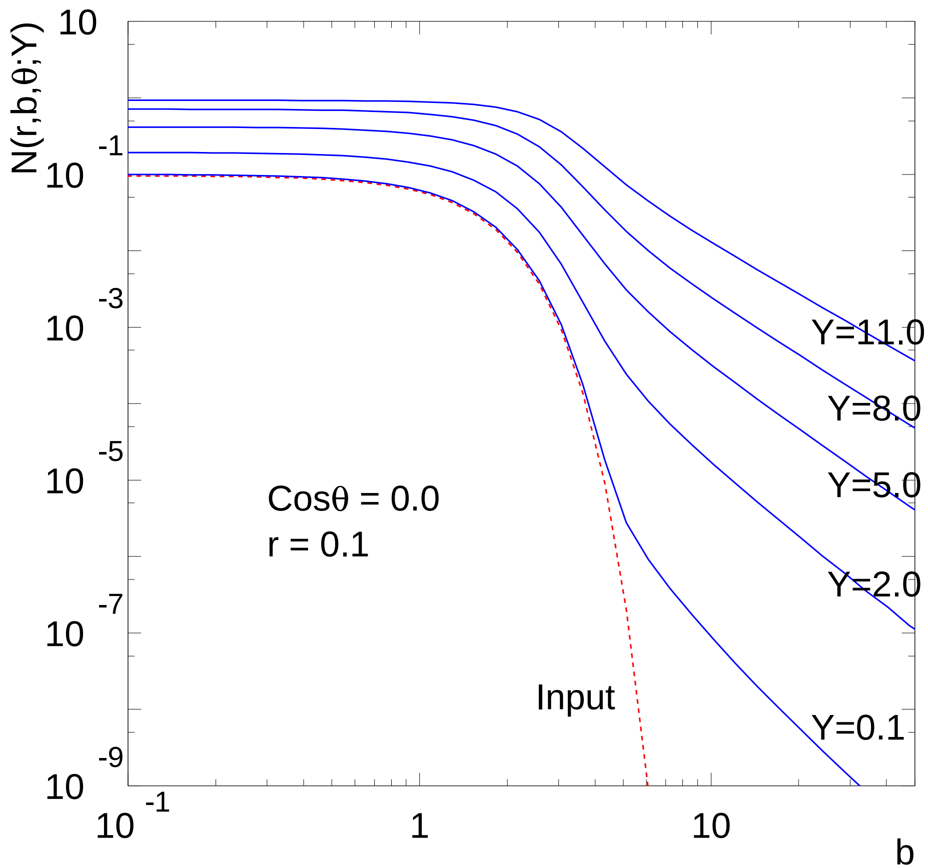

- Froissart bound, $\sigma \propto \ln^2 s$, recovered by non-linear effects? (FIIM, NPA710(01)373; KW, PRD66(02)051502; PLB551(03)311): b-dependence.
- No mass gap $\Rightarrow$ no Froissart expected; initial condition $\propto e^{-Ab}$ for $b \gg$ but a tail $\propto b^{-4}$ develops $\Rightarrow$ regulation of the kernel is demanded.
- Relevant for soft physics and to really determine $Q_s(b)$.

Running coupling:

Solutions of BK with (two upper curves on the left, lower one on the right), and without running coupling for different IR regularizations (B, PLB576(03)115); here y is real rapidity.

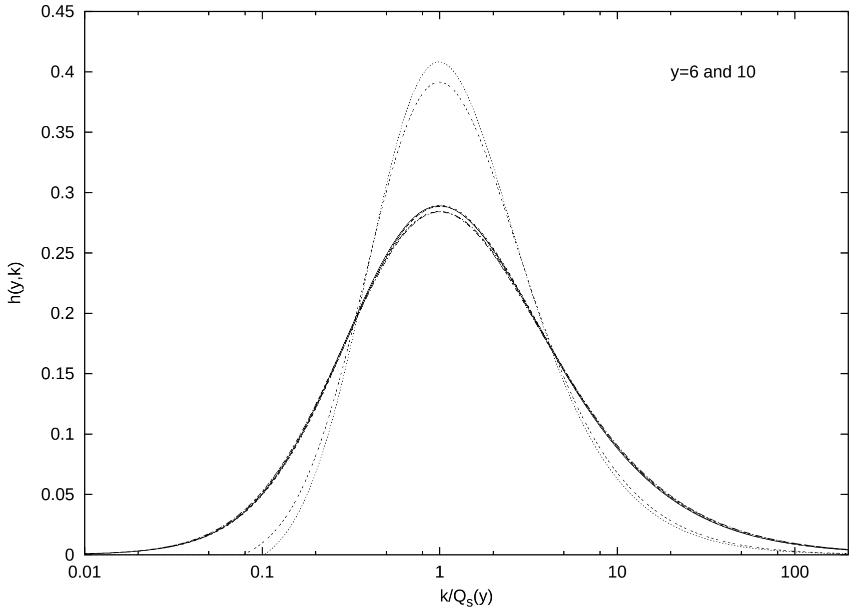

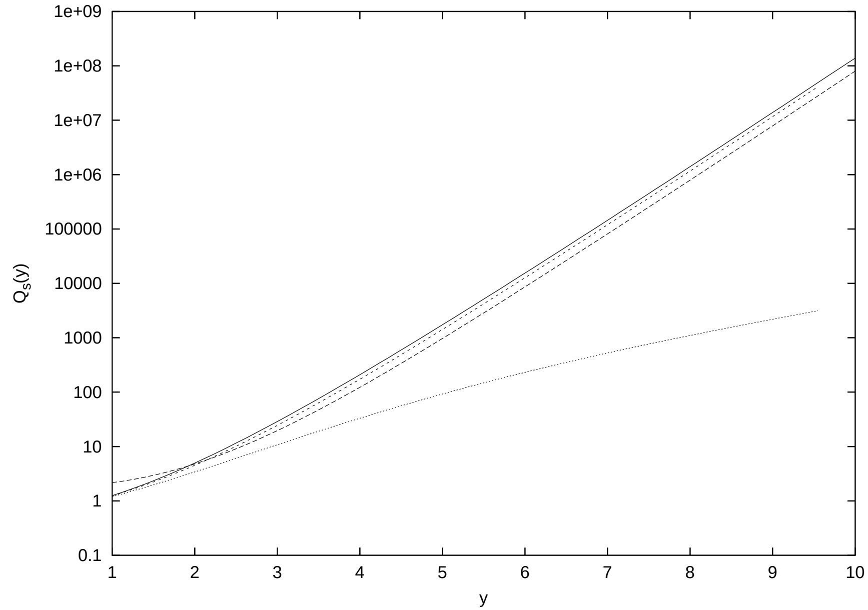

Running coupling:

Solutions of BK with (two upper curves on the left, lower one on the right), and without running coupling for different IR regularizations (B, PLB576(03)115); here y is real rapidity.

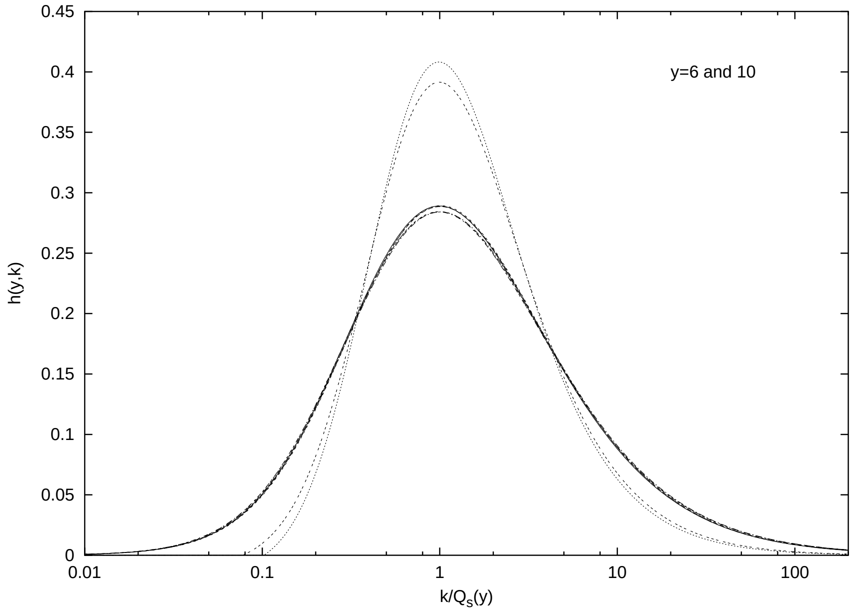

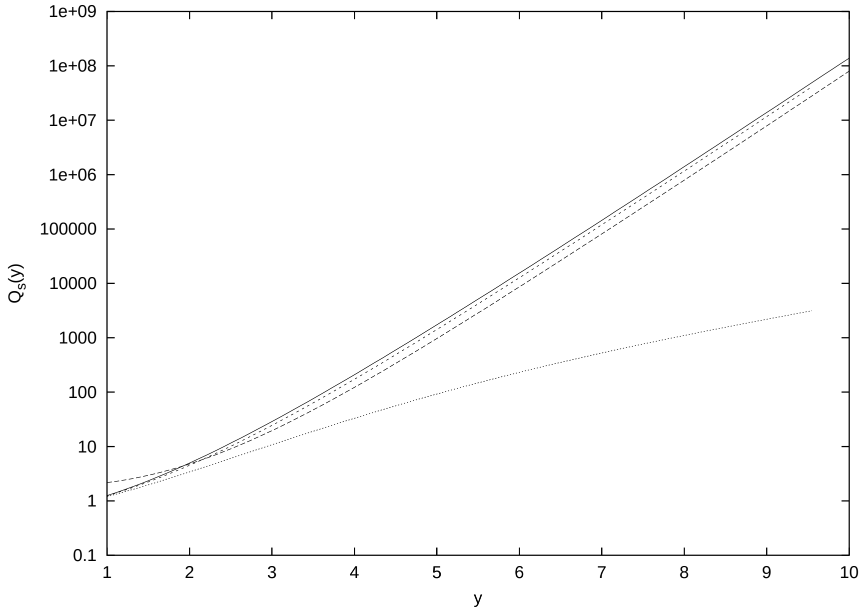

- A scaling function of k/Q_s still appears.

Running coupling:

Solutions of BK with (two upper curves on the left, lower one on the right), and without running coupling for different IR regularizations (B, PLB576(03)115); here y is real rapidity.

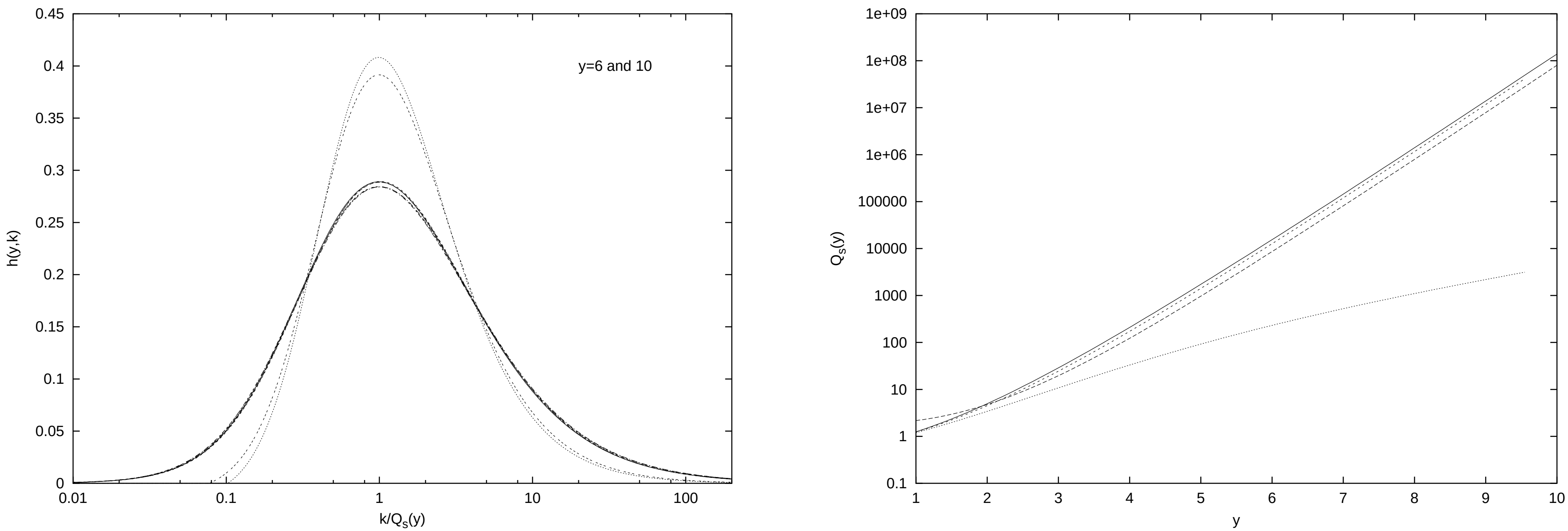

- A scaling function of k/Q_s still appears.
- Better IR and UV behavior ($h = k^2 \nabla_k^2 \phi$).

Running coupling:

Solutions of BK with (two upper curves on the left, lower one on the right), and without running coupling for different IR regularizations (B, PLB576(03)115); here y is real rapidity.

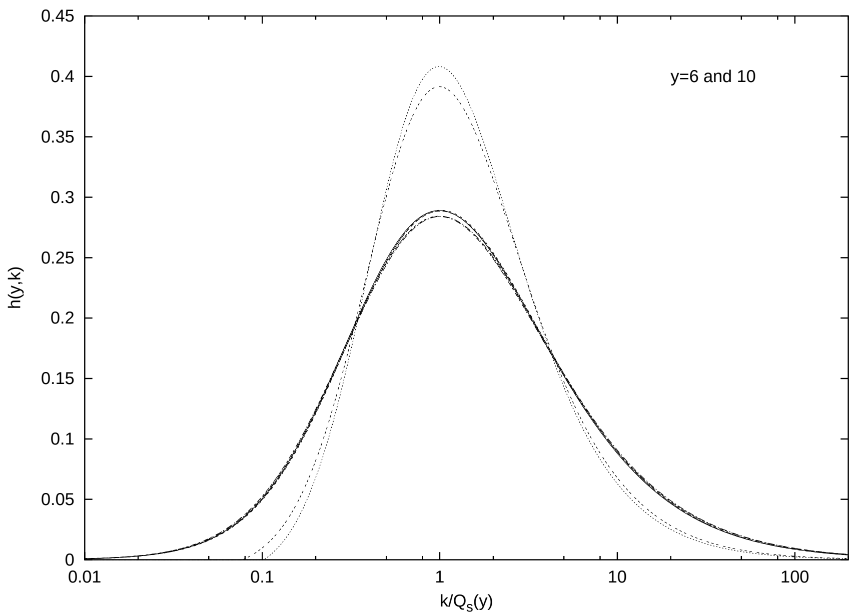

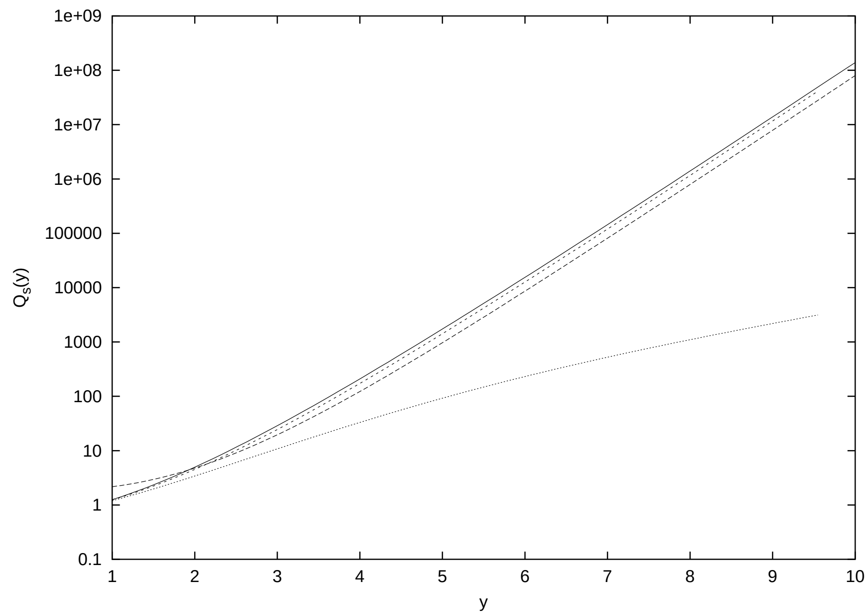

- A scaling function of k/Q_s still appears.
- Better IR and UV behavior ($h = k^2\nabla_k^2\phi$).
- With $Q_s^2(y) \propto \exp{(\Delta y)}$, $\Delta_{\rm rc} \sim \Delta_{\rm fc}/2$ (T, 648(03)293; RW, hep-ph/0309306): much closer to the value $\simeq 0.3$ (for $\alpha_s \sim 0.2$) found in data (GBW, PRD59(99)014017).

Running coupling:

Solutions of BK with (two upper curves on the left, lower one on the right), and without running coupling for different IR regularizations (B, PLB576(03)115); here y is real rapidity.

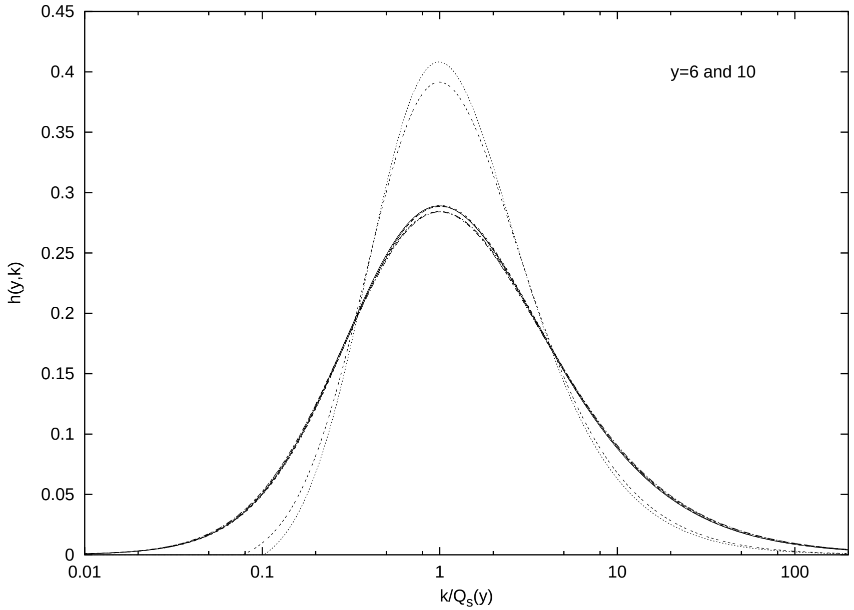

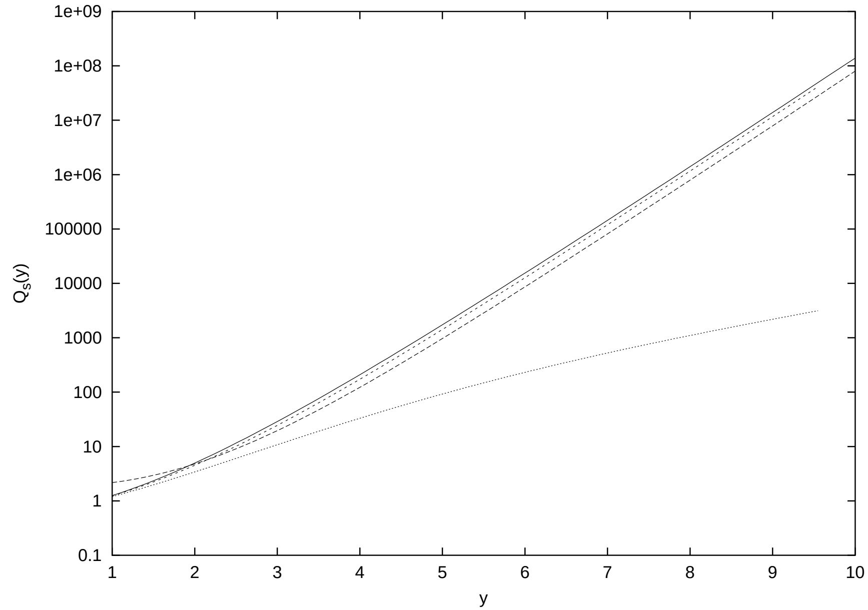

- A scaling function of k/Q_s still appears.
- Better IR and UV behavior ($h = k^2 \nabla_k^2 \phi$).
- With $Q_s^2(y) \propto \exp(\Delta y)$, $\Delta_{\rm rc} \sim \Delta_{\rm fc}/2$ (T, 648(03)293; RW, hep-ph/0309306): much closer to the value $\simeq 0.3$ (for $\alpha_s \sim 0.2$) found in data (GBW, PRD59(99)014017).
- Behavior of Q_s with A in this case? (M, NPA724(03)223); b-dependence? (GKLMN, hep-ph/0401021).

Difference between the average of the correlator of 4 Wilson lines and the factorized ansatz (RW, hep-ph/0309306); here $0 < Y < 2.5$ and $U = W_F$ previously defined.

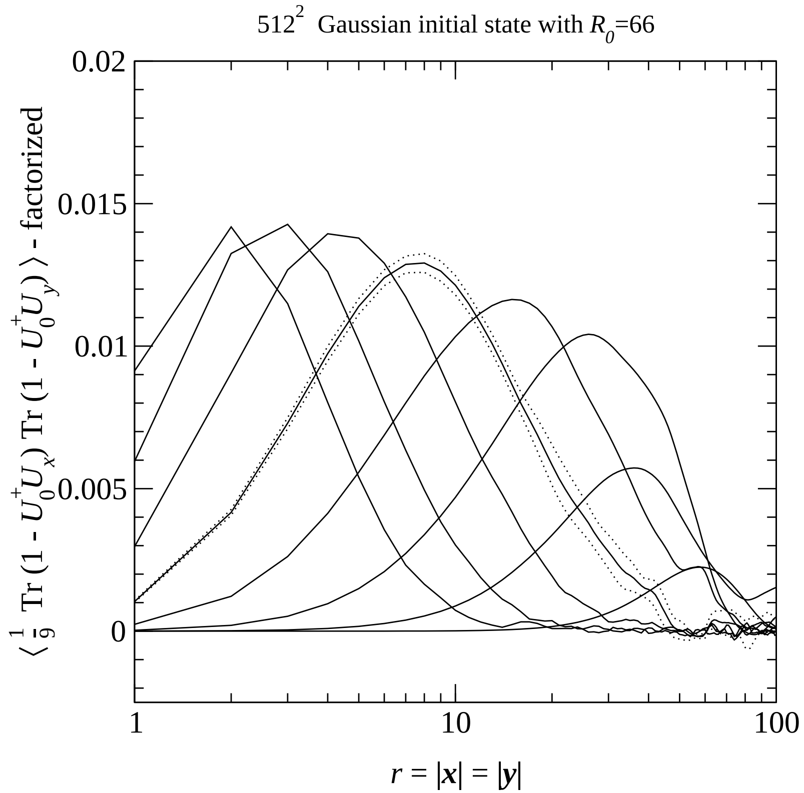

Difference between the average of the correlator of 4 Wilson lines and the factorized ansatz (RW, hep-ph/0309306); here $0 < Y < 2.5$ and $U = W_F$ previously defined.

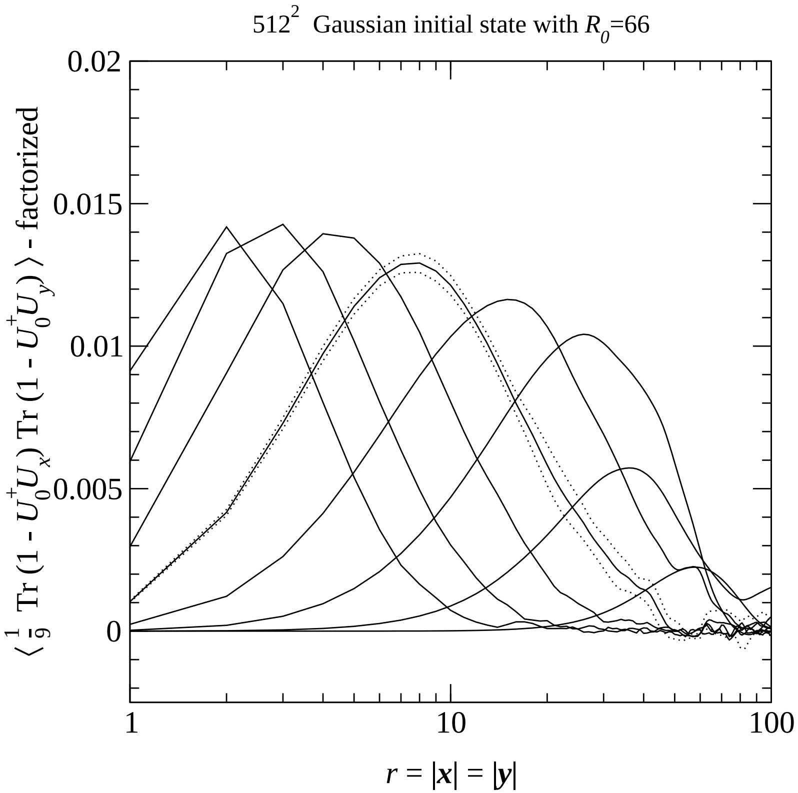

- $\left\langle W_F^\dagger(x_1) W_F(z) W_F^\dagger(z) W_F(x_2) \right\rangle \to \left\langle W_F^\dagger(x_1) W_F(z) \right\rangle \left\langle W_F^\dagger(z) W_F(x_2) \right\rangle$

as in BK implies a loss of fluctuations (IM, NPA730(04)494; MS, hep-ph/0402193).

Difference between the average of the correlator of 4 Wilson lines and the factorized ansatz (RW, hep-ph/0309306); here $0 < Y < 2.5$ and $U = W_F$ previously defined.

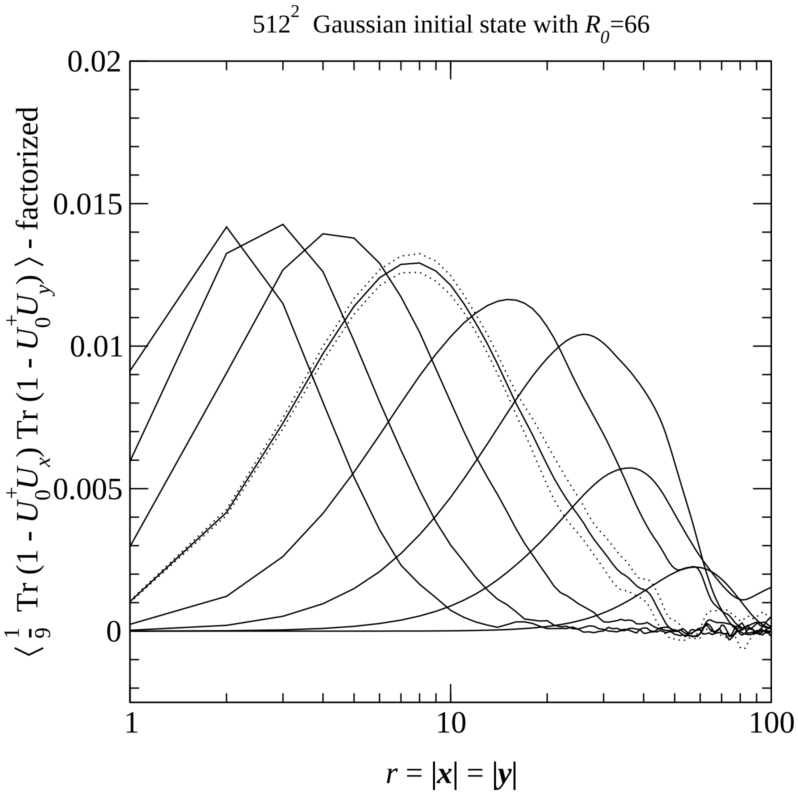

- $\left\langle W_F^\dagger(x_1) W_F(z) W_F^\dagger(z) W_F(x_2) \right\rangle \to \left\langle W_F^\dagger(x_1) W_F(z) \right\rangle \left\langle W_F^\dagger(z) W_F(x_2) \right\rangle$
as in BK implies a loss of fluctuations (IM, NPA730(04)494; MS, hep-ph/0402193).
- Better use full CGC (JIMWLK equation): far more involved.

Difference between the average of the correlator of 4 Wilson lines and the factorized ansatz (RW, hep-ph/0309306); here $0 < Y < 2.5$ and $U = W_F$ previously defined.

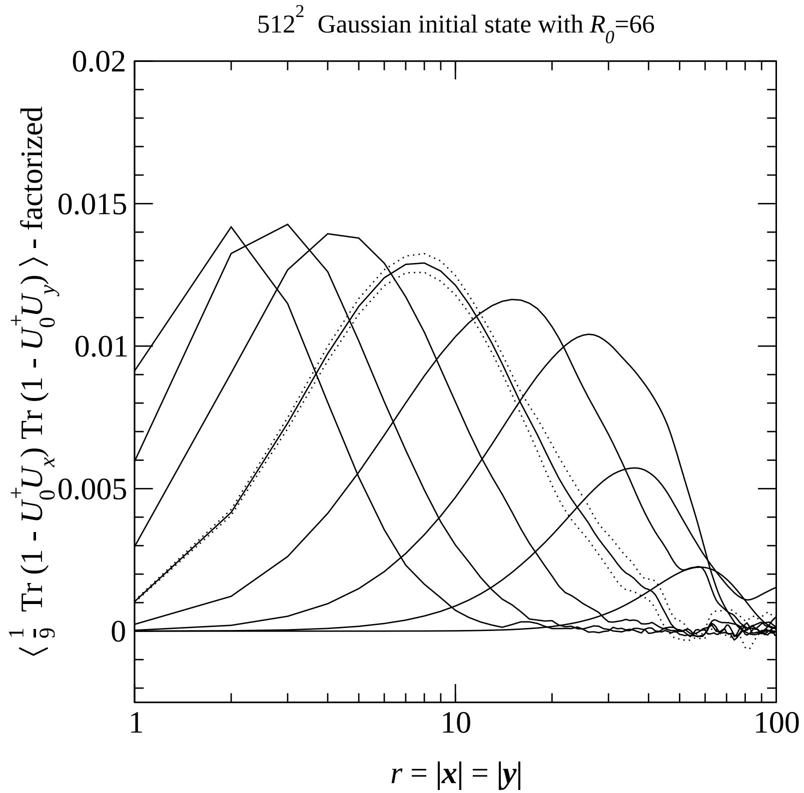

- $\left\langle W_F^\dagger(x_1) W_F(z) W_F^\dagger(z) W_F(x_2) \right\rangle \to \left\langle W_F^\dagger(x_1) W_F(z) \right\rangle \left\langle W_F^\dagger(z) W_F(x_2) \right\rangle$ as in BK implies a loss of fluctuations (IM, NPA730(04)494; MS, hep-ph/0402193).
- Better use full CGC (JIMWLK equation): far more involved.
- This factorization does not seem a large effect (compared to the typical size ~ 1) but maybe crucial to get the correct small-r behavior.

4. Consequences in eA and HIC:

- eA: F_2 and heavy flavor production.
- HIC: Cronin effect.

Just two aspects touched, a huge range of applications is available, see the other mentioned talks.

Note: x is usually *assumed* to be small enough, $< (2m_N R_A)^{-1}$.

eA: F_2 and heavy flavor production:

Néstor Armesto

Results of BK for $F_{2\mathrm{Pb}}$ and charm production in eA collisions (AB, EPJC22(01)351).

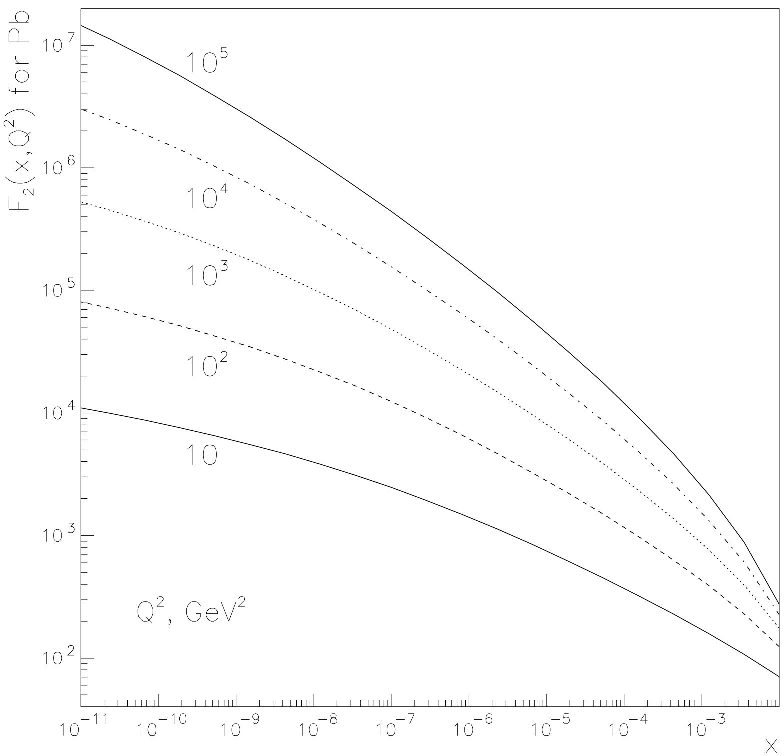

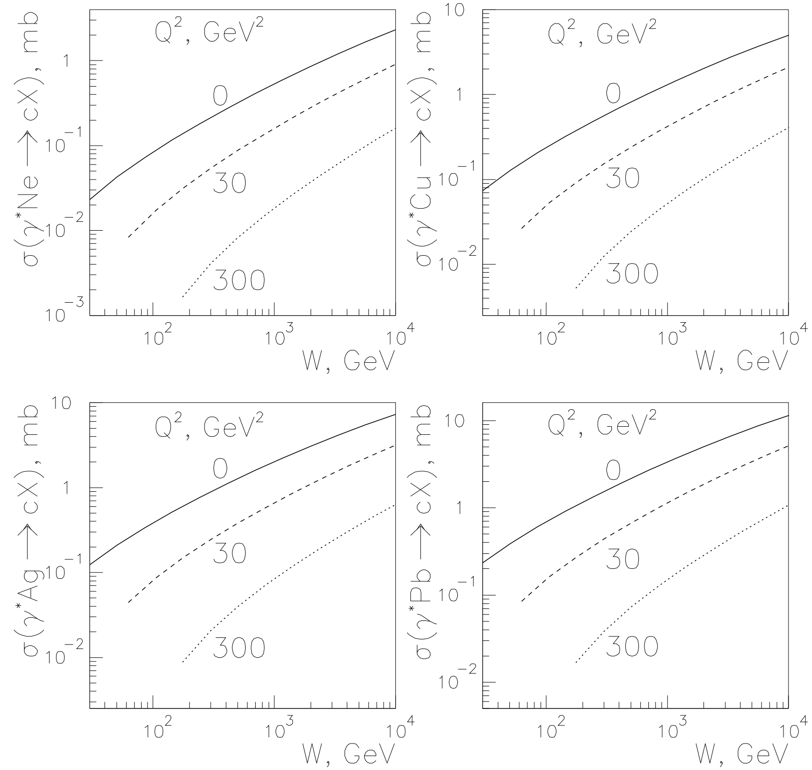

eA: F_2 and heavy flavor production:

Néstor Armesto

Results of BK for $F_{2\mathrm{Pb}}$ and charm production in eA collisions (AB, EPJC22(01)351).

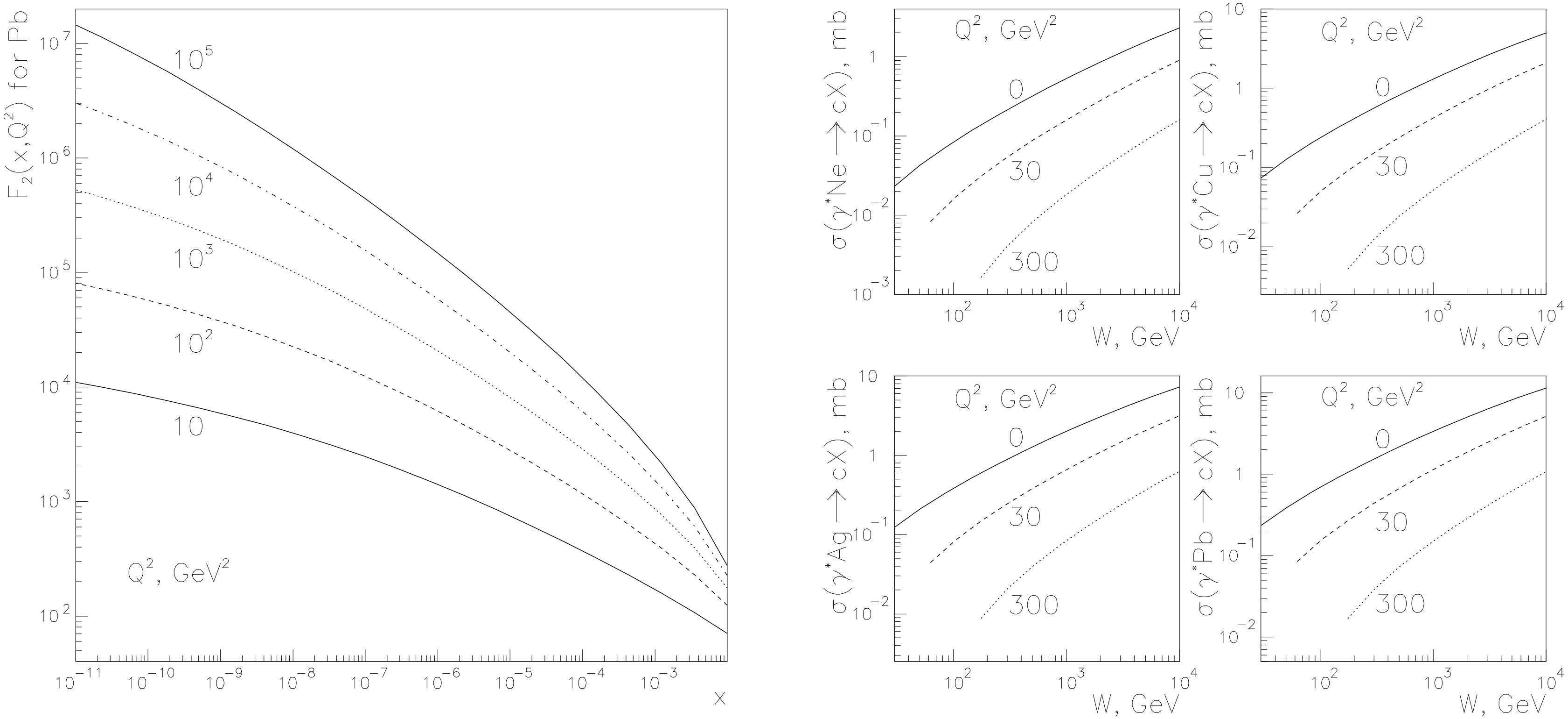

• $F_{2\mathrm{A}}$: slower increase with $1/x$, $\propto \ln^2(1/x)$ (but no b-dependence, so the initial condition determines the b-dependence).

eA: F_2 and heavy flavor production:

Néstor Armesto

Results of BK for $F_{2\mathrm{Pb}}$ and charm production in eA collisions (AB, EPJC22(01)351).

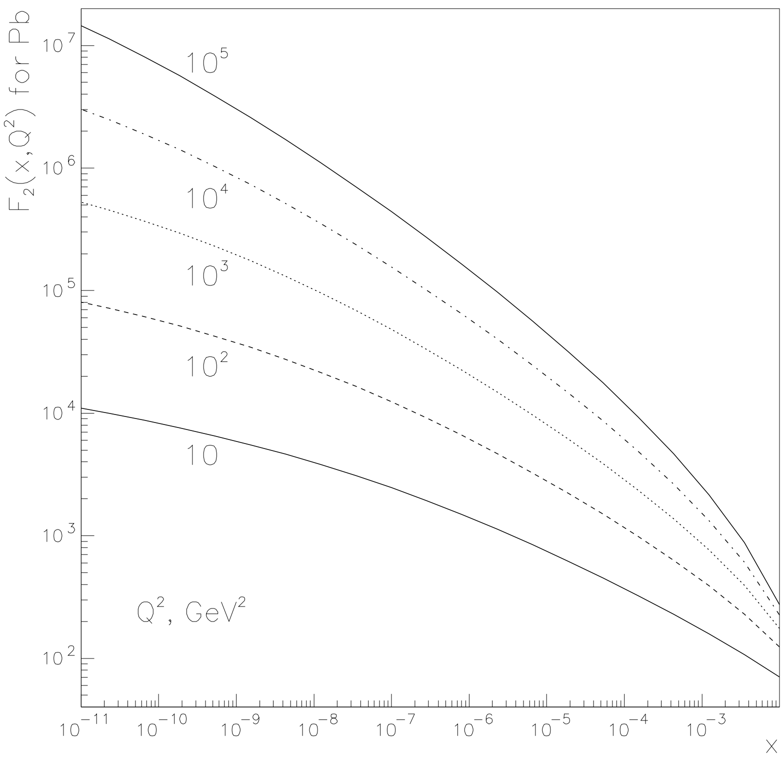

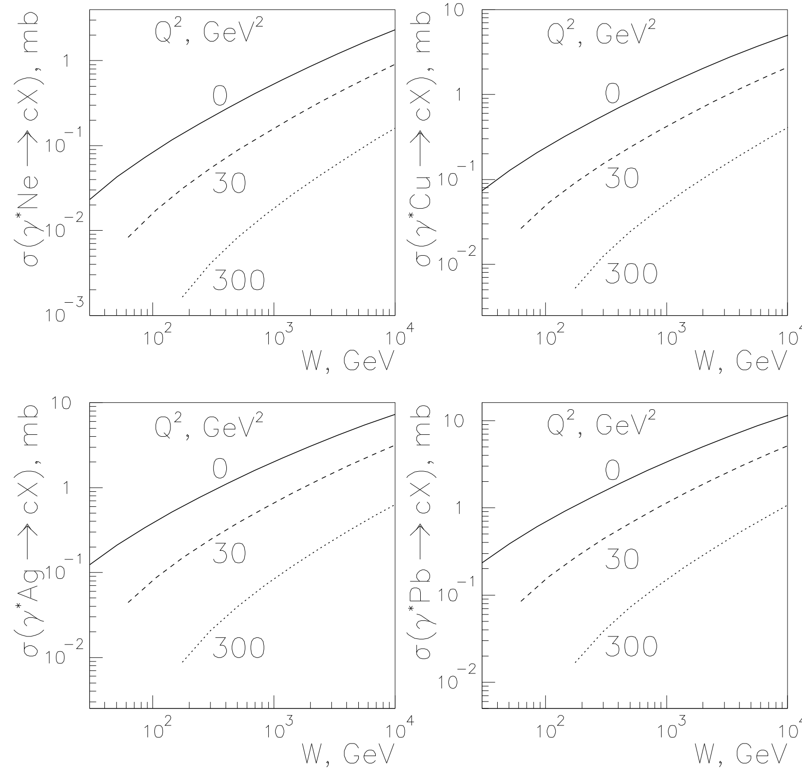

- $F_{2\mathrm{A}}$: slower increase with $1/x$, $\propto \ln^2(1/x)$ (but no b-dependence, so the initial condition determines the b-dependence).
- If $F_{2\mathrm{A}} = A^{\alpha(x,Q^2)} F_{2\mathrm{p}}$, $\alpha \sim 0.9$ for $x \sim 10^{-3}$ and $0.7 \div 0.8$ for $x \sim 10^{-6}$.

eA: F_2 and heavy flavor production:

Results of BK for $F_{2\mathrm{Pb}}$ and charm production in eA collisions (AB, EPJC22(01)351).

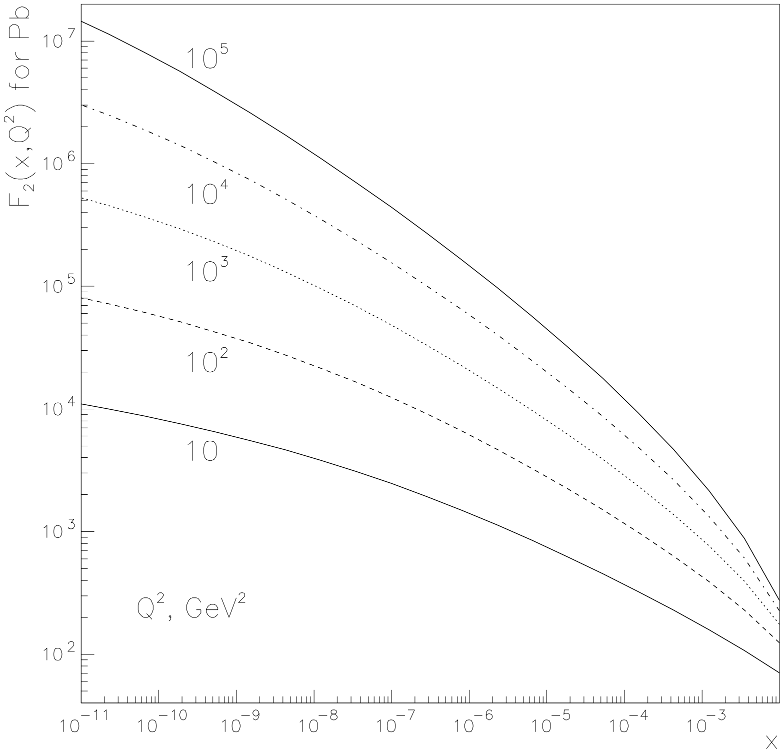

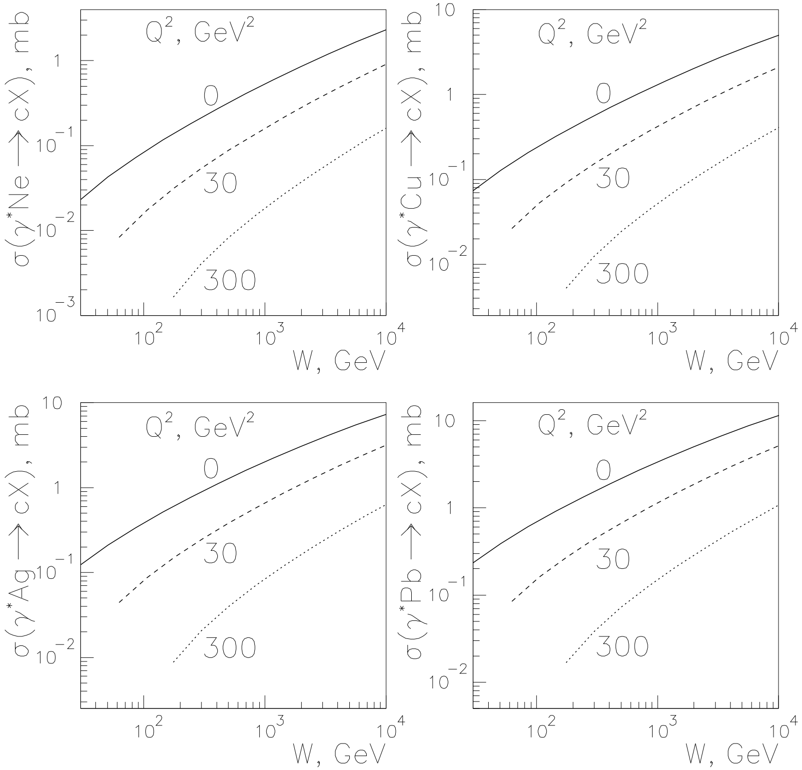

- $F_{2\mathrm{A}}$: slower increase with $1/x$, $\propto \ln^2(1/x)$ (but no b-dependence, so the initial condition determines the b-dependence).
- If $F_{2\mathrm{A}} = A^{\alpha(x,Q^2)} F_{2\mathrm{p}}$, $\alpha \sim 0.9$ for $x \sim 10^{-3}$ and $0.7 \div 0.8$ for $x \sim 10^{-6}$.
- Heavy quark production larger than in collinear factorization (GM, EPJC30(03)387); transverse momenta $\gg$ than the mass are not negligible.

HIC: Cronin effect (I):

$$R_{pA} = \frac{\frac{dN_{pA}}{dyd^2p\,d^2b}}{A^{1/3}\frac{dN_{pp}}{dyd^2p\,d^2b}}, \qquad R_{AA} = \frac{\frac{dN_{AA}}{dyd^2p\,d^2b}}{A^{4/3}\frac{dN_{pp}}{dyd^2p\,d^2b}}.$$

- Gluon spectra in pp, pA or AB are computed using some factorization, $N_g \propto \int f_A\, f_B$ (GLR, PR100(83)1; KM, NPB529(98)451; B, PLB483(00)105; KKT, PRD68(03)094013; BGV, hep-ph/0402256), or classical field simulation (KV, PRL84(00)4307; KNV, NPA727(03)427; L, PRC67(03)054903); hadronization or LPHD is then used. In this way, bulk properties like multiplicities are understood within saturation (KL, PLB523(01)79).

$$R_{pA} = \frac{\frac{dN_{pA}}{dyd^2p\,d^2b}}{A^{1/3}\frac{dN_{pp}}{dyd^2p\,d^2b}}\,, \qquad R_{AA} = \frac{\frac{dN_{AA}}{dyd^2p\,d^2b}}{A^{4/3}\frac{dN_{pp}}{dyd^2p\,d^2b}}\,.$$

- Gluon spectra in pp, pA or AB are computed using some factorization, $N_g \propto \int f_A\, f_B$ (GLR, PR100(83)1; KM, NPB529(98)451; B, PLB483(00)105; KKT, PRD68(03)094013; BGV, hep-ph/0402256), or classical field simulation (KV, PRL84(00)4307; KNV, NPA727(03)427; L, PRC67(03)054903); hadronization or LPHD is then used. In this way, bulk properties like multiplicities are understood within saturation (KL, PLB523(01)79).
- It has been argued (KLM, PLB561(03)93) that large transverse momentum suppression in AuAu at RHIC can be described within saturation. But, if so, it should also be present in dAu at the same rapidity, which is not the case $\Longrightarrow$ final state effects in AuAu.

$$R_{pA} = \frac{\frac{dN_{pA}}{dyd^2p\,d^2b}}{A^{1/3}\frac{dN_{pp}}{dyd^2p\,d^2b}}, \qquad R_{AA} = \frac{\frac{dN_{AA}}{dyd^2p\,d^2b}}{A^{4/3}\frac{dN_{pp}}{dyd^2p\,d^2b}}.$$

• Gluon spectra in pp, pA or AB are computed using some factorization, $N_g \propto \int f_A\, f_B$ (GLR, PR100(83)1; KM, NPB529(98)451; B, PLB483(00)105; KKT, PRD68(03)094013; BGV, hep-ph/0402256), or classical field simulation (KV, PRL84(00)4307; KNV, NPA727(03)427; L, PRC67(03)054903); hadronization or LPHD is then used. In this way, bulk properties like multiplicities are understood within saturation (KL, PLB523(01)79).

• It has been argued (KLM, PLB561(03)93) that large transverse momentum suppression in AuAu at RHIC can be described within saturation. But, if so, it should also be present in dAu at the same rapidity, which is not the case $\Longrightarrow$ final state effects in AuAu.

• The presence (Cronin) or absence of enhancement in the ratios is due to the behavior of gluon distributions just above Q_s (BKW, PRD68(03)054009); other ingredients (e.g. factorization, hadronization,. . .) do not change this qualitative behavior.

$$R_{pA} = \frac{\frac{dN_{pA}}{dyd^2p\,d^2b}}{A^{1/3}\frac{dN_{pp}}{dyd^2p\,d^2b}}, \qquad R_{AA} = \frac{\frac{dN_{AA}}{dyd^2p\,d^2b}}{A^{4/3}\frac{dN_{pp}}{dyd^2p\,d^2b}}.$$

- Gluon spectra in pp, pA or AB are computed using some factorization, $N_g \propto \int f_A\, f_B$ (GLR, PR100(83)1; KM, NPB529(98)451; B, PLB483(00)105; KKT, PRD68(03)094013; BGV, hep-ph/0402256), or classical field simulation (KV, PRL84(00)4307; KNV, NPA727(03)427; L, PRC67(03)054903); hadronization or LPHD is then used. In this way, bulk properties like multiplicities are understood within saturation (KL, PLB523(01)79).
- It has been argued (KLM, PLB561(03)93) that large transverse momentum suppression in AuAu at RHIC can be described within saturation. But, if so, it should also be present in dAu at the same rapidity, which is not the case $\Longrightarrow$ final state effects in AuAu.
- The presence (Cronin) or absence of enhancement in the ratios is due to the behavior of gluon distributions just above Q_s (BKW, PRD68(03)054009); other ingredients (e.g. factorization, hadronization,. . .) do not change this qualitative behavior.
- Initial conditions based on multiple scattering (e.g. Glauber-Mueller or MV) lead to enhancement (JNV, PLB577(03)54).

- Evolution erases the Cronin effect present in the initial condition (AAKSM, PRL92(04)082001; KKT, PRD68(03)094013).

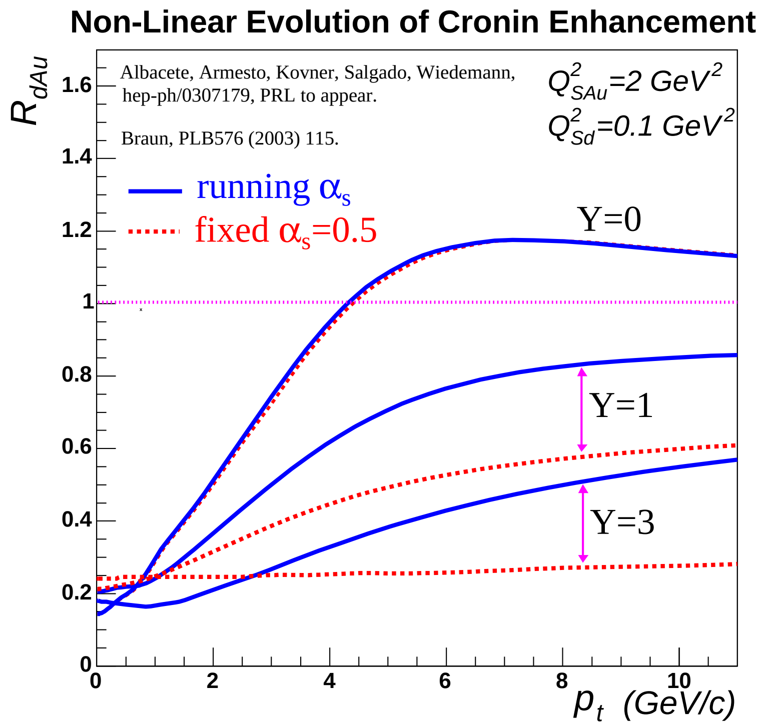

- Evolution erases the Cronin effect present in the initial condition (AAKSM, PRL92(04)082001; KKT, PRD68(03)094013).
- Thus, it predicts its disappearance at forward rapidities at RHIC, seen in data (BRAHMS Coll., nucl-ex/0403005).

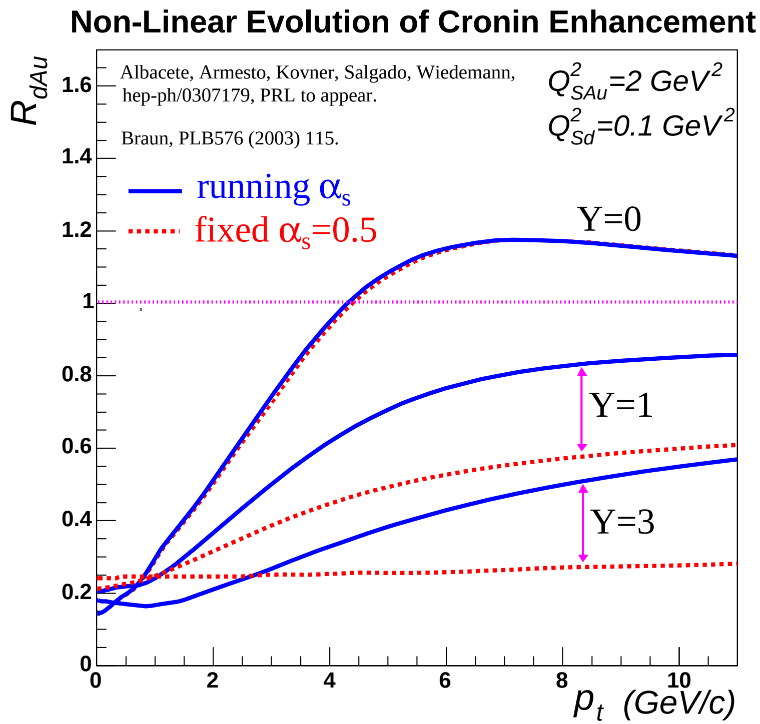

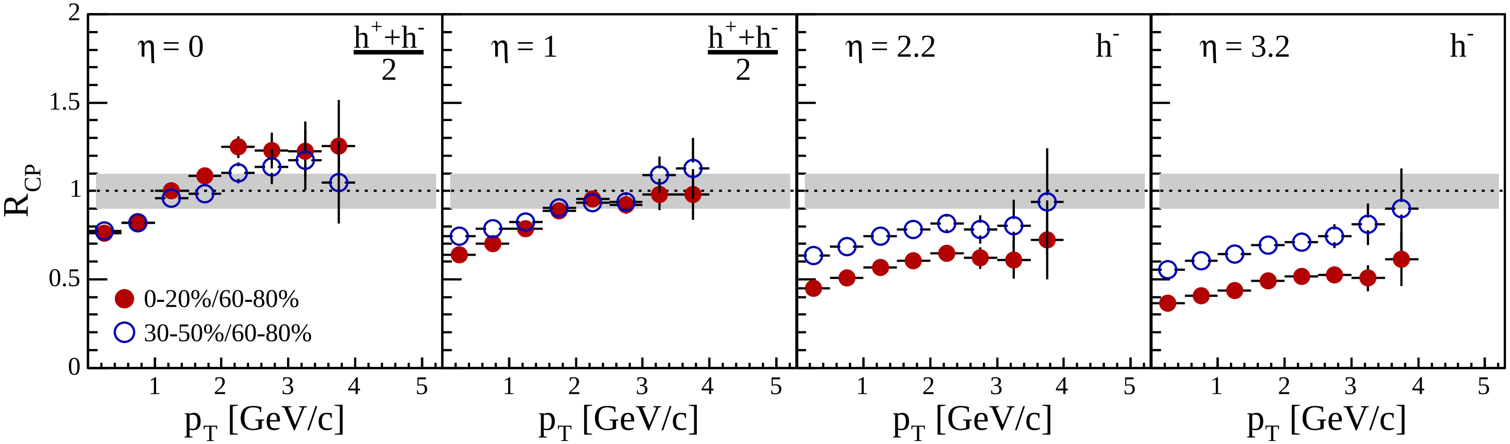

HIC: Cronin effect (II):

- Evolution erases the Cronin effect present in the initial condition (AAKSM, PRL92(04)082001; KKT, PRD68(03)094013).
- Thus, it predicts its disappearance at forward rapidities at RHIC, seen in data (BRAHMS Coll., nucl-ex/0403005).
- No attempt to reproduce data; uncertainties (e.g. fc vs rc, finite energy effects,. . .) still large.

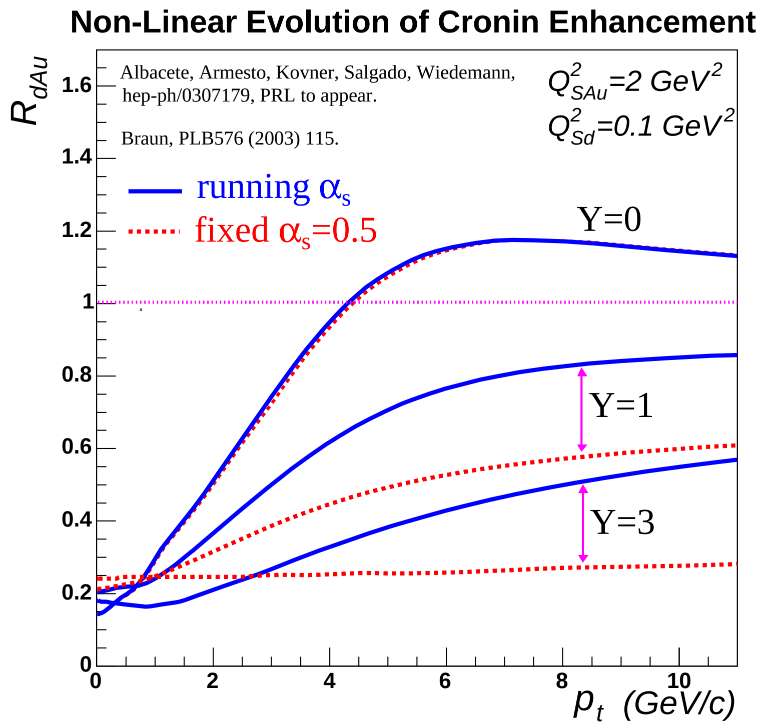

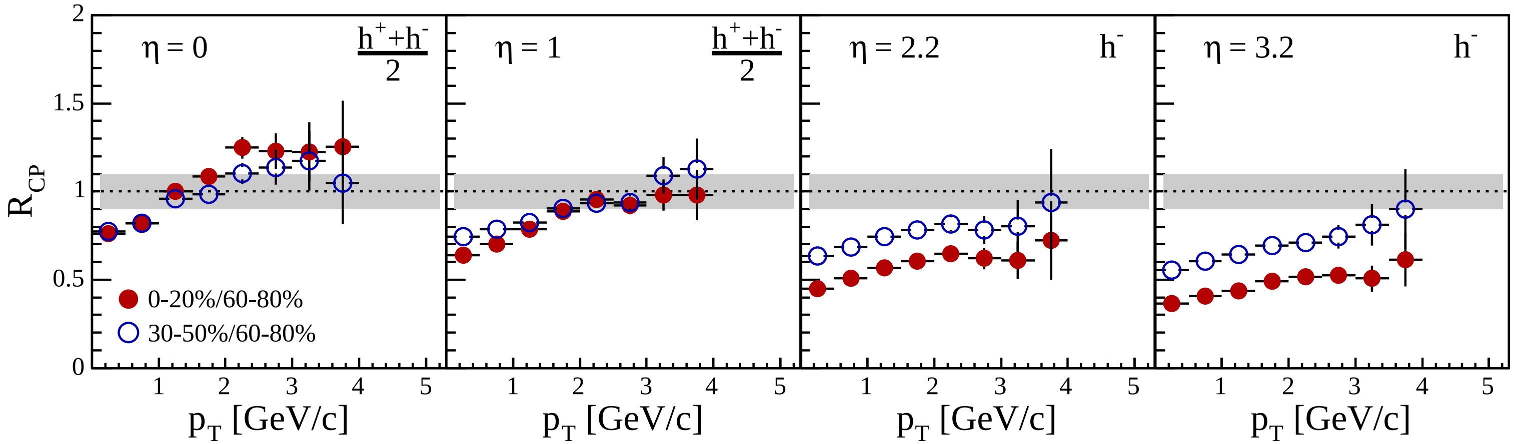

5. Summary:

- Evolution equations in the high parton density, non-linear regime of QCD are available. They are, together with factorization theorems, the key ingredient to compute observables in high-energy collisions involving nuclei.

5. Summary:

- Evolution equations in the high parton density, non-linear regime of QCD are available. They are, together with factorization theorems, the key ingredient to compute observables in high-energy collisions involving nuclei.

- The main features of the solutions of the most widely used tool, the BK equation, are known: integrability, scaling and good IR behavior. Analytical estimates and numerical solutions are available.

5. Summary:

- Evolution equations in the high parton density, non-linear regime of QCD are available. They are, together with factorization theorems, the key ingredient to compute observables in high-energy collisions involving nuclei.

- The main features of the solutions of the most widely used tool, the BK equation, are known: integrability, scaling and good IR behavior. Analytical estimates and numerical solutions are available.

- The inclusion of running coupling and effects beyond BK is under study.

5. Summary:

- Evolution equations in the high parton density, non-linear regime of QCD are available. They are, together with factorization theorems, the key ingredient to compute observables in high-energy collisions involving nuclei.

- The main features of the solutions of the most widely used tool, the BK equation, are known: integrability, scaling and good IR behavior. Analytical estimates and numerical solutions are available.

- The inclusion of running coupling and effects beyond BK is under study.

- These works have already been crucial to establish the large transverse momentum suppression measured in AuAu at RHIC as a final state effect.

5. Summary:

- Evolution equations in the high parton density, non-linear regime of QCD are available. They are, together with factorization theorems, the key ingredient to compute observables in high-energy collisions involving nuclei.
- The main features of the solutions of the most widely used tool, the BK equation, are known: integrability, scaling and good IR behavior. Analytical estimates and numerical solutions are available.
- The inclusion of running coupling and effects beyond BK is under study.
- These works have already been crucial to establish the large transverse momentum suppression measured in AuAu at RHIC as a final state effect.
- Many predictions are available. An eA collider is the cleanest place to study these high parton density phenomena.